

**DEVELOPMENT OF FIBER REINFORCED  
CYLINDRICAL COMPOSITE STRUCTURES BY  
FILAMENT WINDING TECHNIQUE**

**A Thesis Submitted to  
the Graduate School of Engineering and Sciences of  
İzmir Institute of Technology  
in Partial Fulfillment of the Requirements for the Degree of**

**MASTER OF SCIENCE**

**in Mechanical Engineering**

**by  
Mustafa AYDIN**

**December 2019  
İZMİR**

## ACKNOWLEDGMENTS

I would like to give my sincere thanks to my advisor, Prof. Dr. Metin TANOĞLU for his guidance, support, motivation and encouragement during my thesis.

I would like to thank to my labmates Ceren TÜRKDOĞAN, Hatice SANDALLI, Zeynep AY, Gözde ESENOĞLU, Serkan KANGAL, Mehmet Deniz GÜNEŞ, Yusuf Can UZ and Seçkin MARTİN for their help, support and motivation.

I am especially grateful to my colleague, my friend Hikmet Sinan ÜSTÜN for his great contribution.

I am also deeply grateful to Osman KARTAV for his mentoring, invaluable contributions, motivation, support and patience during my whole thesis study.

Lastly but most importantly, I offer sincere thanks to my lovely parents Duygu AYDIN and Özcan AYDIN, my brother Emre AYDIN and Damra Nur ÜSTEL for their great motivation, unprecedented support and endless patience throughout my education.

# ABSTRACT

## DEVELOPMENT OF FIBER REINFORCED CYLINDRICAL COMPOSITE STRUCTURES BY FILAMENT WINDING TECHNIQUE

Fiber reinforced composite structures with superior properties are used for cylindrical structure systems in many application areas nowadays. The major aim of this thesis is development of filament wound composite cylindrical structures with various fiber types on different ply sequence and investigate their mechanical properties. For this purpose, 4 layered glass, carbon and glass/carbon hybrid fiber reinforced cylindrical structures were manufactured with 55 degree winding angle by utilizing filament winding technique. Produced 6 different composite structures have 1 m length and 60 mm inner diameter. Glass/carbon fiber reinforced systems were developed to reduce the cost by reducing carbon fiber usage. Apparent hoop tensile strength and radial compression tests were applied to the manufactured composite structures.

In addition to these studies, two different composite plate with glass fiber and carbon fiber reinforcements were produced by filament winding to investigate glass transition temperature. These plates were manufactured with 4 layered by using the same fiber and matrix as used in the previous tube production. Dynamic mechanical analysis was performed with samples which is sectioned from plates to obtain glass transition temperature.

Consequently, apparent hoop tensile strength test results showed that hoop strength of glass fiber reinforced cylindrical structures can be improved significantly by hybridization. Based on the radial compression test results, deflection of the structures decreases by hybridization.

## ÖZET

### ELYAF TAKVİYELİ SİLİNDİRİK KOMPOZİT YAPILARIN FİLAMENT SARMA YÖNTEMİ İLE GELİŞTİRİLMESİ

Fiber takviyeli kompozitler üstün özelliklerinden dolayı son dönemlerde silindirik yapı sistemlerinde sıklıkla kullanılmaya başlanmış ve önemli bir konuma gelmiştir. Bu çalışmadaki amaç farklı tip fiber ve yönelim kullanılarak hibrit kompozit silindirik yapılar üretmek, bu silindirik yapıların mekanik özelliklerini ve hibridizasyonun etkilerini incelemektir. Bu doğrultuda her bir kompozit yapı 4 katmanlı olacak şekilde 55 derece sarım açısıyla sarılmıştır. 1 metre boyunda 60 mm iç çapa sahip 6 tip farklı kompozit silindirik yapı filaman sarım yöntemi ile üretilmiş, bu silindirik yapılara fiber içeriği, halka çekme testi ve radyal basma testleri uygulanmıştır.

Bu çalışmaların yanında, camsı geçiş sıcaklığını incelemek için cam fiber ve karbon fiber sarılı iki ayrı plaka filaman sarım metodu ile üretildi. Üretilen bu plakalar da tüp sarımındaki ile aynı fiber ve matris kullanılarak 4 kat sarım yapılmıştır. Bu üretimlerden alınan numuneler ile dinamik mekanik analiz yapılmış ve camsı geçiş sıcaklığı incelenmiştir.

Sonuçlar incelendiğinde referans baz alınan cam fiber takviyeli kompozit silindirik yapılara kıyasla hibridizasyon ile mekanik özelliklerin arttığı gözlenmiş ve karbon fiber takviyeli silindirik yapılara kıyasla maliyet azaltılmıştır.

# TABLE OF CONTENTS

LIST OF FIGURES .....	viii
LIST OF TABLES .....	xi
CHAPTER 1. INTRODUCTION .....	1
1.1. Introduction of Composite Materials.....	1
1.2. Manufacturing Techniques of Fiber Reinforced Composite Tubes .....	2
1.2.1. Filament Winding Process .....	3
1.2.2. Roll Wrapping Process .....	6
1.2.3. Pultrusion Process.....	7
1.2.4. Pullbraiding Process .....	8
CHAPTER 2. LITERATURE SURVEY.....	10
CHAPTER 3. EXPERIMENTAL.....	16
3.1. Materials .....	16
3.2. Filament Winding Machine and Support Equipments .....	17
3.3. Manufacturing of Composite Tubes.....	18
3.4. Mechanical Testing of Composite Tubes .....	22
3.4.1. Apparent Hoop Tensile Test.....	22
3.4.2. Radial Compression Test.....	25
3.5. Calculation of Fiber Mass Fraction .....	27
3.6. Manufacturing of Composite Plates .....	28
3.7. Investigations of Thermal Properties of Composite Plates .....	30
3.7.1. Dynamic Mechanical Analysis .....	30
CHAPTER 4. RESULTS AND DISCUSSION.....	31
4.1. Microstructural Properties of Filament Wound Composite Tubes.....	31
4.1.1. Fiber Mass Fraction .....	31
4.2. Thermal Properties of Filament Wound Composite Plates .....	32

4.2.1. Dynamic Mechanical Analysis Results .....	32
4.3. Mechanical Properties of Filament Wound Composite Tubes.....	34
4.3.1. Apparent Hoop Tensile Test Results .....	34
4.3.2. Radial Compression Test Results .....	40
CHAPTER 5. CONCLUSIONS .....	49
REFERENCES .....	51

# LIST OF FIGURES

<u>Figure</u>	<u>Page</u>
Figure 1.1. Composite parts of Airbus A350 XWB .....	1
Figure 1.2. Drive shaft (a), rods of bike frame (b), rocket motor casing (c) .....	2
Figure 1.3. Discontinuous filament winding process .....	4
Figure 1.4. Continuous filament winding process .....	4
Figure 1.5. Schematic representation of the impregnation system .....	5
Figure 1.6. Filament winding patterns .....	6
Figure 1.7. Roll wrapping process of prepreg around the steel mandrel .....	6
Figure 1.8. Manufacturing stages of pultrusion process .....	7
Figure 1.9. Schematic representation of pullbraiding process .....	8
Figure 1.10. Photograph of the pullbraiding process by using carbon fibers .....	9
Figure 2.1. Glass fiber composite ring sample and split-disk test fixture with sample ..	11
Figure 2.2. Compressive strength and modulus values for different winding angles.....	13
Figure 3.1. Photo of continuous carbon fiber bobbin (a), Photo of continuous glass fiber bobbin (b) .....	16
Figure 3.2. Filament winding machine and tensioner with carbon fiber roving.....	17
Figure 3.3. Photo of resin bath during the manufacturing of glass fiber reinforced composite tube .....	18
Figure 3.4. Filament winding process of G/G/G/C composite tube .....	19
Figure 3.5. Filament winding process of G/G/G/G composite tube .....	19
Figure 3.6. Curing process of glass fiber wound tube .....	20
Figure 3.7. Manufactured composite tubes by using filament winding technique .....	20
Figure 3.8. Schematically representation of composite tube .....	21
Figure 3.9. 55° winding angle of wound composite tube .....	22
Figure 3.10. Schematic representation of split disk test setup .....	23
Figure 3.11. Dimensions of ring test specimens .....	23
Figure 3.12. Sectioned filament wound ring specimens before apparent hoop tensile test .....	24
Figure 3.13. Composite ring specimens were inserted split disks for apparent hoop tensile test.....	25

<b><u>Figure</u></b>	<b><u>Page</u></b>
Figure 3.14. Schematic representation of test setup .....	25
Figure 3.15. Test setup of radial compression test .....	26
Figure 3.16. Radial test specimens which are sectioned from filament wound composite structures.....	27
Figure 3.17. Aluminum plate was wound by teflon film.....	29
Figure 3.18. Manufacturing of carbon fiber wound plate (a), manufacturing of glass fiber wound plate .....	29
Figure 3.19. DMA testing machine .....	30
Figure 4.1. Floating carbon fibers after the hydrogen peroxide addition, glass fibers and carbon fibers are together after drying .....	31
Figure 4.2. Dynamic mechanical analysis result of carbon fiber wound plate specimen	33
Figure 4.3. Dynamic mechanical analysis result of glass fiber wound plate specimen..	33
Figure 4.4. Force-displacement curves of G/G/G/G wound composite ring specimens during split disk test .....	36
Figure 4.5. Force-displacement curves of C/C/C/C wound composite ring specimens during split disk test .....	36
Figure 4.6. Force-displacement curves of C/G/G/G wound composite ring specimens during split disk test .....	37
Figure 4.7. Force-displacement curves of C/G/C/G wound composite ring specimens during split disk test .....	37
Figure 4.8. Force-displacement curves of C/C/C/G wound composite ring specimens during split disk test .....	38
Figure 4.9. Force-displacement curves of glass-carbon Filament Hybrid (FH) wound composite ring specimens during split disk test .....	38
Figure 4.10. Failure modes of the specimens after apparent hoop tensile strength test .	40
Figure 4.11. Force-displacement curves of G/G/G/G wound composite tubes under radial compression .....	43
Figure 4.12. Force-displacement curves of C/C/C/C wound composite tubes under radial compression .....	43
Figure 4.13. Force-displacement curves of C/G/G/G wound composite tubes under radial compression .....	44
Figure 4.14. Force-displacement curves of C/G/C/G wound composite tubes under radial compression .....	44



<b><u>Figure</u></b>	<b><u>Page</u></b>
Figure 4.15. Force-displacement curves of C/C/C/G wound composite tubes under radial compression .....	45
Figure 4.16. Force-displacement curves of glass-carbon Filament Hybrid wound composite tubes under radial compression .....	45
Figure 4.17. Average force-displacement curves of whole produced composite tubes under radial compression .....	46
Figure 4.18. Radial compression test specimen under the compression load.....	47
Figure 4.19. Sectioned filament wound composite samples after compression test.....	47

## LIST OF TABLES

<b><u>Table</u></b>	<b><u>Page</u></b>
Table 2.1. Results of hoop tensile strength based on different winding angles.....	11
Table 3.1. Mechanical properties of resin and reinforcement materials.....	17
Table 3.2. Stacking sequences and average thicknesses of each produced structures....	21
Table 4.1. Average fiber weight ratios of sectioned composite tube specimens .....	32
Table 4.2. Test results of filament wound composite plate .....	32
Table 4.3. Tensile properties of G/G/G/G wound ring specimens .....	34
Table 4.4. Tensile properties of C/C/C/C wound ring specimens .....	34
Table 4.5. Tensile properties of C/G/G/G wound ring specimens.....	34
Table 4.6. Tensile properties of C/G/C/G wound ring specimens.....	35
Table 4.7. Tensile properties of C/C/C/G wound ring specimens .....	35
Table 4.8. Tensile properties of Filament Hybrid (FH) wound ring specimens.....	35
Table 4.9. Average apparent hoop tensile strength values of composite ring structures	39
Table 4.10. Compressive properties of G/G/G/G wound composite tubes .....	41
Table 4.11. Compressive properties of C/C/C/C wound composite tubes .....	41
Table 4.12. Compressive properties of C/G/G/G wound composite tubes.....	41
Table 4.13. Compressive properties of C/G/C/G wound composite tubes.....	42
Table 4.14. Compressive properties of C/C/C/G wound composite tubes .....	42
Table 4.15. Compressive properties of glass-carbon Filament Hybrid (FH) wound composite tubes.....	42
Table 4.16. Average compressive properties of filament hybrid wound composite tubes .....	46

# CHAPTER 1

## INTRODUCTION

### 1.1. Introduction of Composite Materials

In this century, demand of superior materials which have high quality is increased with new technological developments. For this reason, composite materials have revealed and improved step by step. Composite materials are the combination of at least two different materials with unique properties. These unique and superior properties such as high specific strength and elastic modulus, low density, long life time and high corrosion resistance made composites a serious rival for other traditional engineering materials as steel, aluminum, titanium alloys.

These materials have enormous usage areas as aircrafts, automobiles and marine industry to decrease consumption of fuel. Glass fiber reinforced composites mostly used for automotive industry while carbon fiber is the main reinforcement material for aerospace industry. Moreover, it has a crucial effect on military requirements due to their light, durable and strong properties. For instance, new manufactured aircrafts are made from composite materials. Most of the parts of Airbus A350 as fuselage, wings and stabilizers are manufactured by using prepreg composites. Figure 1.1 shows the body and composite structures of the airplane which is consisted of 55 % composite pieces.

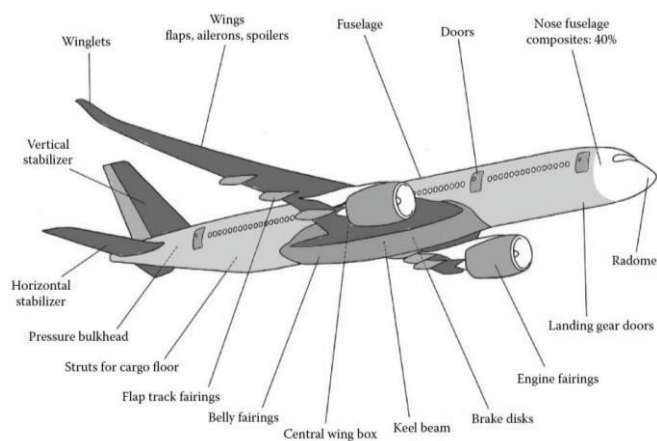


Figure 1.1. Composite parts of Airbus A350 XWB

## 1.2. Manufacturing Techniques of Fiber Reinforced Composite Tubes

Mechanically advanced composite tubes are becoming important part of manufacturing industry. Application areas of composite tubes are increasing day by day. Developing light weight and strong composites is important for automotive, aerospace, defense and marine industries to improve fuel efficiency. Irrigation systems and food production systems are used for transmission of water or chemical fluids and nutrition storage for instance, chemical resistant pipes, tank and silo production, pressurized vessels as LPG or CNG tank.

Moreover, composite tubes are used due to their superior properties which are high corrosion resistance, high durability, fatigue properties, low cost, low maintenance. Drive shaft, ballistic missile, rocket motor casing and space shuttle as shown in Figure 1.2. are examples of application areas of composite tubes.

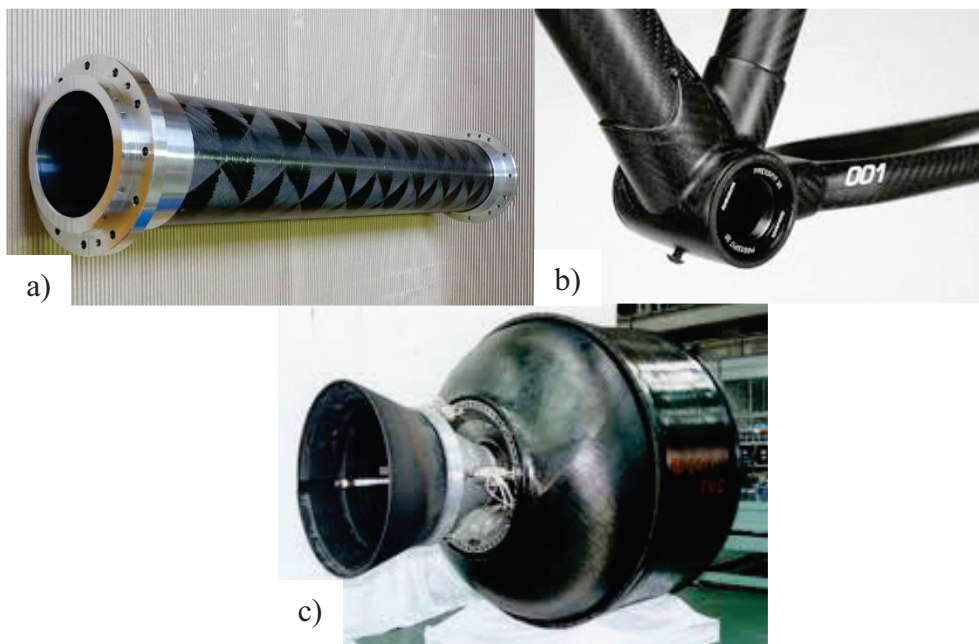


Figure 1.2. Drive shaft (a), rods of bike frame (b), rocket motor casing (c)

Different production methods are used in order to obtain various types of wound composite tubes. Manufacturing of composite tubes are significantly important to obtain complex parts depends on enormous demand from composite industry. Aerospace and aircraft industry are used delicate manufacturing methods so as to come into accurate

dimensions. Increased necessity of product diversity and demand of less production costs are resulted in revealed of new manufacturing methods. There are four different manufacturing methods of fiber reinforced composite tubes as roll wrapping, pultrusion, pullbraiding and filament winding.

### **1.2.1. Filament Winding Process**

Filament winding is used as an impactful fabrication process of composite hollow parts which is usually cylindrical shaped products as drive shaft and closed-end structures as pressure vessel that is used for aerospace industry and chemical plant (Harrison 2000). Filament winding technique has two different methods which are continuous (reciprocal) and discontinuous process (AWWA 1999). In the discontinuous method, continuous fibers are used (Rafiee 2013a). On the other hand, chopped, continuous fibers are rolled onto the mandrel which is endless band in the continuous method. Schematic representation of discontinuous and continuous methods is shown in Figure 1.3 and Figure 1.4, respectively.

A pattern of the composite tube is determined by using simulation software which is managed CNC filament winding machine. Predetermined model of composite structure demonstrates whether feasible for production or not. The rolling process of over the mandrel is carried out with two different methods which are pre-impregnated fibers and fibers that is immersed in the resin bath during winding.

Filament winding technique have advantages and disadvantages. High strength, modulus and fiber fraction are some basic advantages of filament winding process. If complex mandrel shape is required, the manufacturing will be harder, so this is one of the disadvantages of filament winding process.

In the wet filament winding process, reinforcement materials which are continuous fibers as E-glass, S-glass, carbon, aramid and hybrid roving and chopped fibers, matrix materials as epoxy, polyester, vinyl ester and polyurethane resins are used. In addition, prepreg (pre-impregnated) materials as towpreg are preferred due to their superior delicate properties. These materials are laid on mandrel after that only curing process are applied. Towpreg decreases complexity of production and cost of manufacturing.

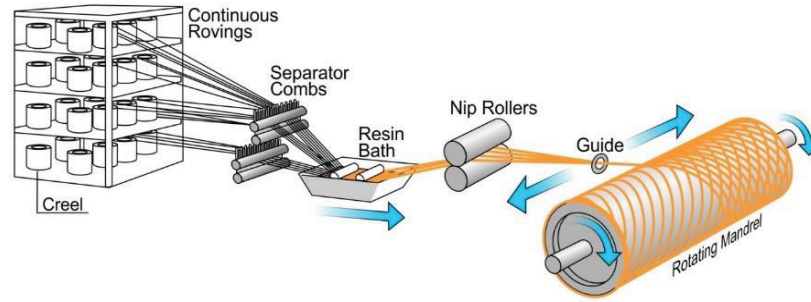


Figure 1.3. Discontinuous filament winding process

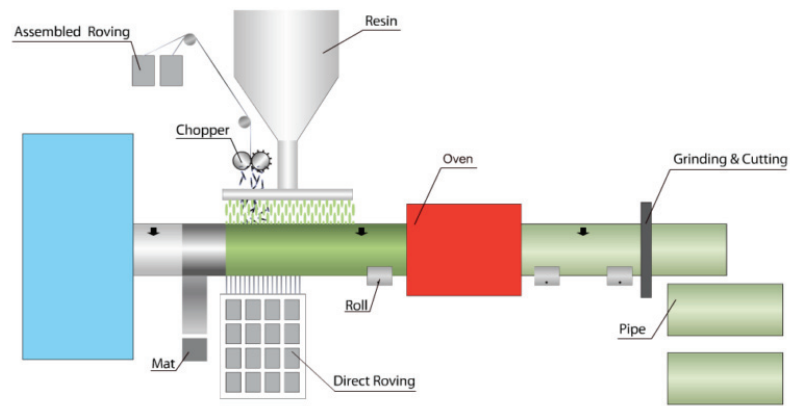


Figure 1.4. Continuous filament winding process

Tension device which is known as tension-regulating system or tensioner is held fiber roving and applies to tension force over the fiber. Tension of fiber is vital to the excessive control of filament winding machine during winding. Ideal tension level of tensioner is determined with type of fiber and winding pattern. Decreasing the fiber tension is led to openness and dislocations between fiber alignments. It is caused lower structural properties. Increasing the fiber tension considerably improved fiber volume fraction of the fiber wound composite structure (Gonzalez Henriquez and Mertiny 2018). Mechanical properties of the composite structures are directly increased with increasing fiber volume ratio. Uniform structure is ensured with correct fiber alignment thanks to tensioner.

Transmission of fibers is controlled by using pulley which is stated between tensioner and resin bath. Staying together of fibers is important for clean production before impregnation.

Resin bath is filled with pre-prepared resin system. The resin bath is used to control resin impregnation of fiber by using immersion method or the fibers pass over the rotating drum. Depends on the manufacturing method temperature of the resin bath is adjustable. This adjustment is related with gelling temperature of resin and application temperature of resin impregnated fibers. Adjustment of temperature of resin bath is critically important by the reason of increasing temperature into the resin bath is lead to changing viscosity. Increasing viscosity of liquid resin result in regional aggregation and decreasing adhesion capability on filament.

An additional part of the resin bath provides that control of fiber volume fraction to increase the mechanical properties of the composite structure. Resin gathering on drum is arranged by using adjustable doctor blade in resin impregnation systems. Moreover, the void content of composite tube is decreased by using doctor blade which prevents bubbles and decreases size of bubbles. Schematic representation of resin bath is shown in Figure 1.5 (Harrison 2000).

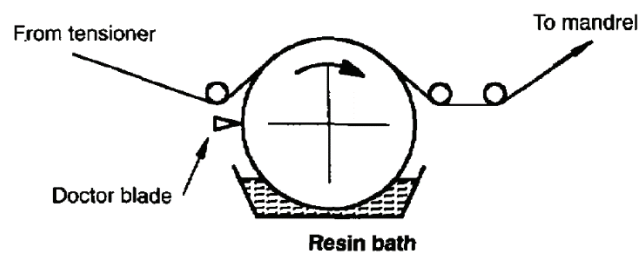


Figure 1.5. Schematic representation of the impregnation system  
(Source: Harrison 2000)

Winding angle is adjusted by using angular movement of robot head. Helical winding, circumferential winding and polar winding are three major winding patterns as shown in Figure 1.6 (Sofi, Neunkirchen, and Schledjewski 2018). The filament by using CNC controlled filament carrier is laid down on the mandrel with predetermined angle. Those type of winding systems depends on the usage area and prediction of mechanical properties. For instance, pressure vessels which is for storage system wound with optimum winding angle as  $54.7^\circ$  (Taib et al. 2006).

In the circumferential winding, fibers are perpendicularly laid on the mandrel by almost  $90^\circ$  degrees. It is generally known as hoop winding (Quanjin et al. 2017). Hoop winding has great contribution on the internal pressure tests. Lower angle winding as

helical and polar provide higher axial or longitudinal stress values. Angle of the polar winding is provided by wrapping the fiber one end to other end of the pressure vessel. It is not possible to wind  $0^\circ$ . In addition, low angle winding has critical problems as slipping due to decreasing friction value between surface of mandrel and resin impregnated fibers. As compared hoop winding with helical and polar winding show more precision quality.

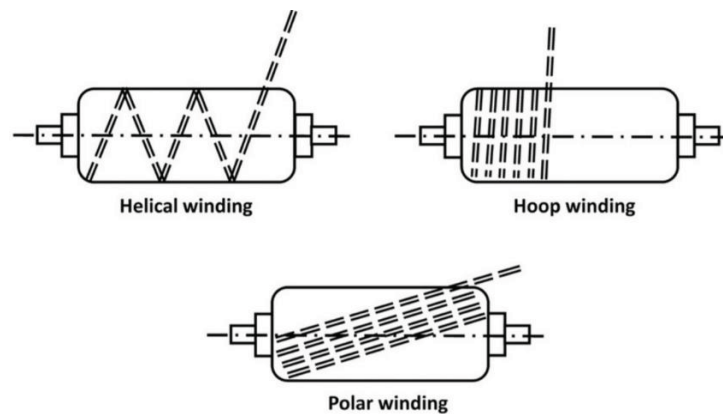


Figure 1.6. Filament winding patterns

### 1.2.2. Roll Wrapping Process

Roll wrapping is another type of manufacturing process and useful to obtain high quality circular shaped parts. In the roll wrapping process, carbon or glass prepreg which is known as a pre-impregnated fiber is laid down around the mandrel by using rolling machine. Roll wrapping method is illustrated schematically in Figure 1.7.

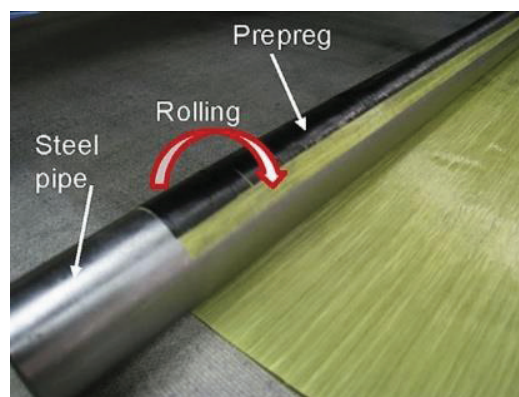


Figure 1.7. Roll wrapping process of prepreg around the steel mandrel  
(Source: Kim et.al., 2011)



A prepreg is wrapped onto a mandrel with tension. The outer diameter of the mandrel determines the inner diameter of the final tube. After the curing process, mandrel is removed from composite tube (Kim, Yoon, and Shin 2011).

Usage of prepreps in order to produce composite tubes drastically increases durability of products due to their high resin and fiber proportion and minimum bubble level. Adequate and optimum impregnated resin level is brought about these results.

### 1.2.3. Pultrusion Process

Pultrusion name comes from pulling and extrusion and used to manufacture fiber reinforced polymer profile which is a hollow part. Pultrusion is a continuous process that ensures dimensional accuracy at cross-section and continuous length (Joshi 2012). Dry, continuous reinforcement materials as fiber roving are passed through a resin bath. Then impregnated fibers are pulled forward to heated die in order to cure and form. After the curing and forming, the composite profile is extracted from die with pulling system. The endless profile is kept shape after curing process and is transmitted to cutter by pulling force. Produced profiles are sectioned by utilizing cutter. Pultrusion method is illustrated schematically in Figure 1.8. (Marco and Gallegos 2014).

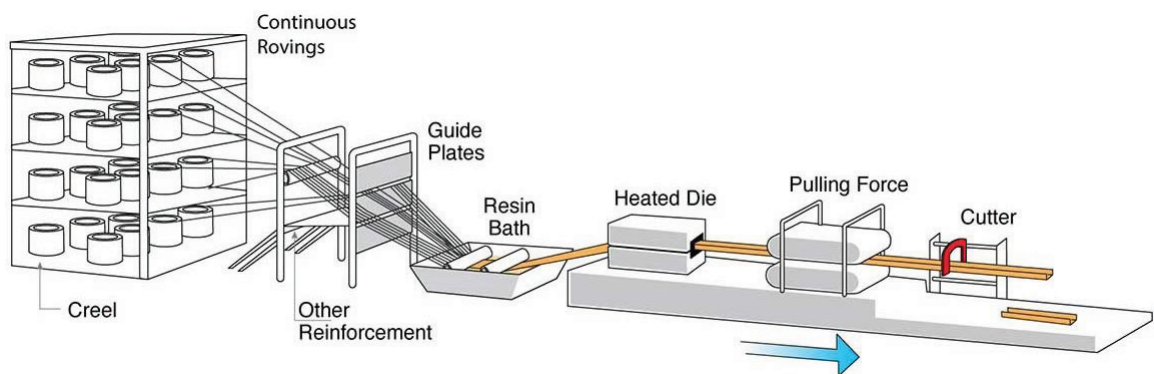


Figure 1.8. Manufacturing stages of pultrusion process

Pultrusion is high effective method for continuous manufacturing. Decreasing cost of resin and fiber, easy to machine, endless production capability, higher fiber to volume ratio are advantages of pultrusion process. Pultrusion is a cheaper process than

filament winding and roll wrapping. Manufacturing of complex shaped composite products and profile which has thin cross-section are improbable in this process.

### 1.2.4. Pullbraiding Process

Pullbraiding has two steps as fiber braiding machine and pultrusion machine as shown in Figure 1.9. Difference from the pultrusion is that the fibers are not directly pass through the resin bath, fibers are braided together onto a mandrel. Fiber braiding is performed with different angles for each layer. After the braiding, process is continued similarly. Braided fibers are pulled into the heated die which is used for impregnation, forming and curing.

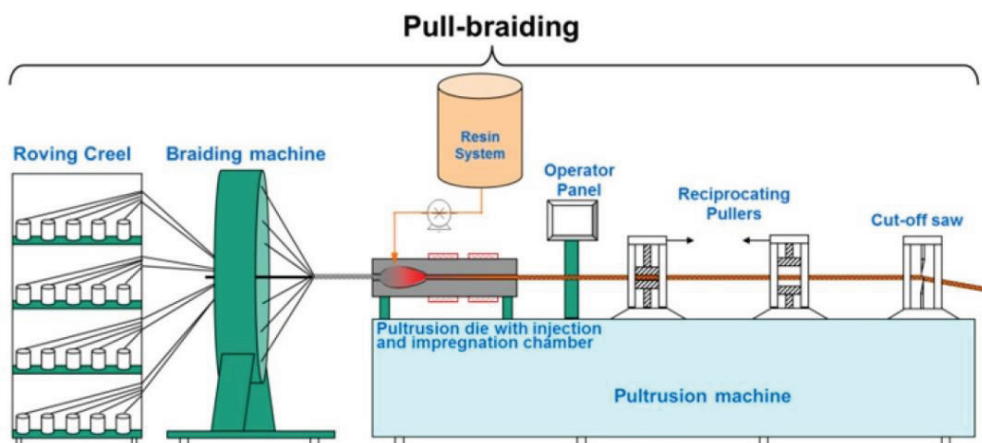


Figure 1.9. Schematic representation of pullbraiding process (Source:Bezerra et al.)

Higher mechanical property, superior surface quality, equality through cross-section and higher fiber volume fraction are expected features of produced hollow parts by using pullbraiding (Bezerra et al. 2015).

High production demand, cost-effective part requirements and decreasing the consumption of fuel are significantly important circumstances for automobile, aerospace and marine industries which are the composite profile utilizers. Figure 1.10. shows cylindrical hollow composite part manufacturing.



Figure 1.10. Photograph of the pullbraiding process by using carbon fibers

## CHAPTER 2

### LITERATURE SURVEY

Cylindrical structures have been used for carriage, storage and power transmission within aerospace, marine, automotive industries and majorly for piping systems. Pipelines that are recently developed requires high specific strength, low weight, and high corrosion resistance (Rafiee 2013). Composite materials have been introduced to the piping systems due to their superior properties such as high specific strength and low weight which make them easier for transportation and high corrosion resistance which provides longer life compared to conventional engineering materials such as steel (Rousseau, Perreux, and Verdière 1999).

Composite piping systems can carry fluids such as water, oil, and gas with the lowest rate of loss since their inside surface quality is better as compared to conventional materials. During the carriage of fluids, the primary requirement for pipes is to be able to bear the internal pressure caused by fluids. According to the international AWWA Standard (AWWA 1999) for fiberglass pressure pipe, composite pipes can be able to carry an internal pressure which is two times of their working pressure (Rafiee 2013b). Therefore, several studies were carried out to measure the internal pressure resistance of composite pipes. Tarakcioglu (2005) studied the fatigue failure behavior of  $[\pm 55^\circ]_4$  glass/epoxy composite pipes manufactured by filament winding technique with  $\pm 55^\circ$  winding angle, under internal pressure. Various load levels 30, 35, 40, 50, 60 and 70 % of ultimate tensile strength were applied to the pipes and whitening, leakage and final failure levels were observed finally. Whitening was observed initially followed by leakage and failure of the pipe was observed finally. Winding angle and other parameters such as tension level and winding speed might have a significant effect on the mechanical properties of the filament wounded cylindrical structures. Moreover, in this study mechanical properties of composite pipes were found as a result static internal pressure test as 405 MPa. Martins, et al. (2014) conducted a numerical/experimental study to investigate the failure pressure of composite pipes with four different winding angles, i.e.;  $[\pm 45^\circ]_4$ ,  $[\pm 55^\circ]_4$ ,  $[\pm 60^\circ]_4$ ,  $[\pm 75^\circ]_4$ .

Experimental and numerical results were correlated, and it was revealed that the pipes with  $\pm 55^\circ$  winding angle exhibited the highest failure pressure. Effect of different winding angle on the mechanical properties of composite pipes was also studied by Kaynak et al. (2005). Since it is easier to perform as compared to internal pressure test, apparent hoop tensile strength (HTS) test was applied by the split disc method according to ASTM D 2290-00 (2003) standard. In Figure 2.1. the sectioned composite ring test specimen and test fixture is shown. It was found that hoop tensile strength increased with winding angle in contrast to internal pressure test.



Figure 2.1. Glass fiber composite ring sample and split-disk test fixture with sample  
(Source: Srebrenkoska, Risteska, and Mijajlovikj 2015)

Srebrenkoska, (2015) carried out a similar study with composite pipes with  $\pm 10^\circ$ ,  $\pm 45^\circ$ ,  $\pm 90^\circ$  winding angles and based on the apparent HTS test results,  $\pm 90^\circ$  composite pipes showed the highest results (Srebrenkoska, Risteska, and Mijajlovikj 2015). Increased HTS values are apparently seen in Table 2.1. From the results of the apparent hoop tensile test, tensile strength of  $\pm 90^\circ$  filament wound specimens are approximately 3.3 times larger than  $\pm 45^\circ$  filament wound specimen.

Table 2.1. Results of hoop tensile strength based on different winding angles  
(Source: Srebrenkoska, Zhezhova, and Naseva 2015)

	Sample Designation	Weight (g)	Width (mm)	Thickness (mm)	$F_{max}$ (N)	Tensile strength (MPa)	Winding angle ( $^\circ$ )
1	1-1	42,2	13,97	3,18	1600	18,00	10
	1-2	43,0	13,85	3,14	1250	14,34	
	1-3	43,7	14,00	3,14	1759	20,00	
2	2-1	53,6	14,01	3,18	25000	280,57	45
	2-2	53,8	13,9	3,16	24225	275,76	
	2-3	53,8	14,01	3,16	24400	275,57	
3	3-1	52,8	14,06	3,64	94500	923,24	90
	3-2	52,8	14,12	3,64	90250	877,97	
	3-3	53,8	14,12	3,65	93000	902,25	

Rosenow (1984) studied cylindrical composite tubes under uniaxial and biaxial loading. This study shows that  $54.7^\circ$  is the optimum angle for closed-end tubes and  $75^\circ$  is for open-end tubes.

Diniz Melo et al. (2011) studied both short time hydraulic pressure and apparent HTS tests and they also performed numerical analysis. Experimental test results showed that apparent HTS and short time hydraulic pressure test results were close to the each other, and they were correlated with numerical results. Rafiee et. al. (2013) used the short time hydraulic failure pressure test to determine the HTS of glass fiber reinforced composite pipes and compare the results with the actual apparent HTS values. Although there was no significant difference between both results, the author claimed that apparent HTS test is better since the test is carried out until the final ply of the composite pipe ruptures.

During transportation, installation, and operation, composite pipes and pressure vessels may be subjected to various loadings such as dynamic impact, static axial, radial compression and bending, etc. (Mertiny, Ellyin, and Hothan 2004). Crushing behavior of composite pipes was investigated by axial compression test (Mertiny, Ellyin, and Hothan 2004), (Kim, Yoon, and Shin 2011). Composite pipes were manufactured by wrapping the prepreg material on an aluminum mandrel, and the effect of different type of fibers (carbon and aramid) was investigated by Kim, Yoon, and Shin (2011). It was found that the carbon fiber-based pipes exhibited the highest compressive strength as compared to those with aramid fibers. In addition to the effect of fiber type, Jia et al. (2013) investigated the effect of winding angle on compressive strength, and consequently, it was found that  $\pm 20^\circ$  showed maximum results as compared to those with the higher winding angles.

Perillo et al. (2014) aimed in their study to make a material characterization of composite tubes basically. Variables are type of fiber and type of resin. Glass fiber-vinyl ester and carbon fiber-epoxy composite pipes are manufactured by  $89^\circ$  winding angle and tested with split disk test method and biaxial. Fiber volume fraction of glass-vinylester and carbon-epoxy composites were found 45.7 % and 61.5 %, respectively. As seen in the literature investigation, the filament winding process doesn't provide exact fiber volume ratio between materials.

Composite pipes might be used to operate underground, and therefore the pipes may be subjected to loading in the radial direction. If this radial earth load during the operation is known, extend of deflection can be calculated using pipe stiffness which is

measured by radial compression test (ASTM D2412-02 Standard 2009). Kannan, Kalaichelvan, and Sornakumar (2015) applied the radial compression and apparent hoop tensile strength tests on composite pipes which were manufactured with  $\pm 45^\circ$  winding angle and had an average thickness of 5 mm. Maximum percentage of deflection was found to be 35 and authors concluded that the composite pipes developed are suitable for piping systems.

Jia et al. (2013) aimed to find reinforced end and unreinforced end effect on axial compression test with using 4 different winding angles as  $20^\circ$ ,  $40^\circ$ ,  $60^\circ$  and  $90^\circ$ . CFRP tubes by end reinforcing demonstrated higher compressive values than unreinforced end composite tubes. Decreasing winding angle resulted with increasing compressive strength. Modulus of composite tubes linearly decreased with increased angle. Figure 2.2. demonstrates compressive strength and modulus depend on the winding angles.

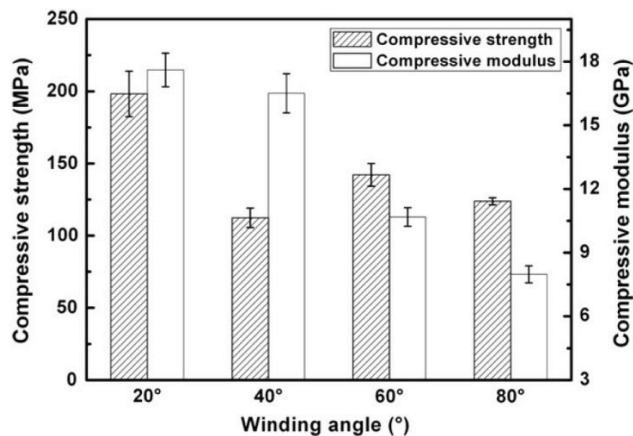


Figure 2.2. Compressive strength and modulus values for different winding angles

Correct modeling of composite materials and mechanical testing aided by Finite Element (FE) method became increasingly important as it may reduce design, manufacturing and quality control costs in piping systems. While dealing with composite failure and damage, one needs to accurately define damage initiation criteria which defines when first ply failure (FPF) occurs in the composite structure. This is followed by damage evolution in composite structures as structural integrity continues beyond FPF until the final collapse of the composite. Several studies in the literature evaluated both experimental and numerical results and validated FE models that feature FPF criteria and

progressive damage analysis beyond FPF. Barsoum and Al Ali (2015) addressed shortcomings of ring test setups and developed a novel testing method for determining the tangential stress-strain behavior of metal pipes. FE method was utilized for evaluating tangential stress across the ring test specimen and effect of frictional behavior of the specimen with D-blocks during testing. It is found that the proposed testing method shows decent agreement both experimentally and numerically with similar test methods. In another study, Almeida et al. (2017) studied the radial compression test (ASTM D2412) and finite element analysis to evaluate pipe stiffness and % of deflection. FE model featured continuum damage mechanics (CDM) model which is capable of damage prediction and evolution utilizing and energy-based stiffness degradation. Results showed that the deflection was measured as about 21 %, which is even less than the value mentioned in the previous study and the progressive damage model was in a good agreement with experimental results. Ellul and Camilleri (2015) investigated the effect of manufacturing variances on the stress-strain behavior, and final structural failure of filament wound cylindrical composite structures. A progressive failure algorithm was developed, featuring a material property degradation method for damage evolution. Manufacturing divergences such as thickness and voids were also implemented into FE model and thoroughly investigated. It was revealed that the progression of failure and the stress-strain response was found to be strikingly dependent on implemented manufacturing variances. A recent study by Rafiee, Torabi, and Maleki (2018) investigated the structural failure of filament wound composite tubes subjected to internal pressure. Hashin failure criterion was selected for determining FPF and two different progressive damage approaches, ply-discount method and CDM were compared with experimental results. Results indicated that ply-discount method underestimates final burst pressure of tubular structures while more accurate estimating was achieved using the CDM approach.

After the literature survey, most of the researches are exploring these effects as inner diameter of the tubes 60 mm or 70 mm, average thickness of whole tubes between 1 mm and 3 mm, 4 or 6 layers are generally used, optimum winding angle which is changed depend on the requirements is  $55^\circ$ , reinforcement materials which are glass fiber, carbon fiber and kevlar are used for composite tube systems, although epoxy is mostly preferred matrix material, polyester is also used. Various mechanical tests that are implemented to the fiber wound composite tubes are apparent hoop tensile, axial and radial compression, burst pressure and three-point bending tests.



As reported within the literature, several mechanical tests such as internal pressure, compression and apparent hoop tensile strength were utilized to investigate the effect of pipe manufacturing parameters. However, there is a lack of information in the literature about the effects of hybrid fibers on the mechanical properties of composite pipes. In this regard, the aim of the present study is to develop the filament wound composite pipes using various type of fiber, with improved mechanical performance and reduced cost. Glass, carbon, and glass/carbon fiber hybrid reinforced composite pipes were manufactured with winding angle of  $[\pm 55^\circ]_4$  using filament winding technique. Apparent hoop tensile strength test which is preferred rather than internal pressure and short time hydraulic failure pressure tests and radial compression tests were performed to calculate the hoop tensile strength, stiffness and percentage deflection of the pipes.

## CHAPTER 3

### EXPERIMENTAL

#### 3.1. Materials

In this study, to evaluate and analyze the mechanical properties of composite cylindrical structures six different cylindrical structures were manufactured by using two different types of continuous filaments which are glass and carbon fiber. Glass fibers (1200 Tex FWR6) were ensured from Şişe Cam Inc. (Turkey), and carbon fibers (800 tex A-49) were ensured from DowAksa Inc. (Turkey). Both continuous fibers were selected especially for the filament winding process. The photo of the continuous fibers which was utilized in the study is shown in Figure 3.1.

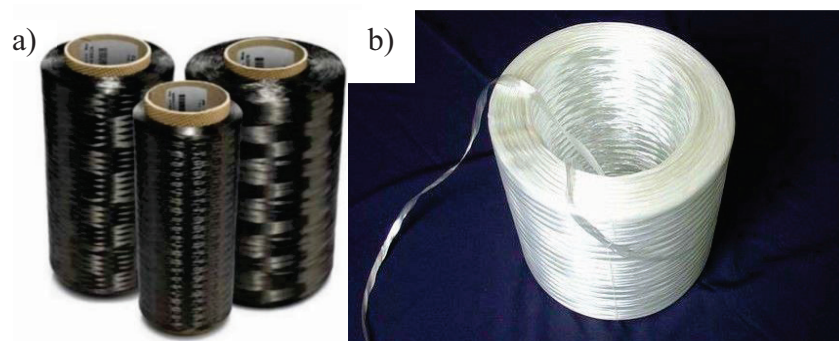


Figure 3.1. Photo of continuous carbon fiber bobbin (a), Photo of continuous glass fiber bobbin (b)

A three-component epoxy system (Huntsman™ Inc.) was chosen as matrix material. Epoxy resin was used as a matrix material. The epoxy system comprises Araldite™ MY740 epoxy resin, Araldur™ MY918 curing agent and DY062 accelerator. Mixing ratio between epoxy resin and curing agent is 85 % (weight ratio). Accelerator is added into pre-mixed resin and hardener system by 0.5–2.5 % wt. The epoxy system is convenient for the filament winding, wet laminating, and pultrusion process and it was recommended by the manufacturer (Araldite resin system). The epoxy system has a low-

viscosity which is a crucial property for the manufacturing method. The mechanical properties of this resin and reinforcement materials are given in Table 3.1.

Table 3.1. Mechanical properties of resin and reinforcement materials

Properties	Glass fiber	Carbon fiber	Epoxy resin
Young's Modulus [GPa]	73	250	3.6
Strain [%]	1.5	2	2.0
Density [g/cm <sup>3</sup> ]	2.6	1.79	1.16
Tensile Strength [MPa]	2400	4900	61

### 3.2. Filament Winding Machine and Support Equipments

Filament winding process is highly automatic technique. This untouched technique is prevented any improper manufacturing thanks to capability of movement in different axis. Fibermak Composites Inc. filament winding machine was utilized to produce filament wound composite tubes. Filament winding machine has a 4-axis working capacity. This high working capacity of machine increases production of complex structures and system works with CADWIND™ software.



Figure 3.2. Filament winding machine and tensioner with carbon fiber roving

The machine has supporting equipment which is known as a tensioner to hold and give tension to the fiber roving. Tensioner has four fiber carriage capability as shown in Figure 3.2. Moreover, the tensioner can be able to tense four fiber roving with chosen tension level at same time during filament winding. On the other hand, curing oven is another exclusive equipment to cure filament wound composite parts.

### 3.3. Manufacturing of Composite Tubes

The fiber reinforced cylindrical composite structures were manufactured by using filament winding technique. Winding angle, length of composite tube, number of layers, speed of winding and tension level are base properties of the winding process. Due to delicate manufacturing, winding was first simulated by utilizing a software (CADWIND™). Simulation is rather user friendly and demonstrates whether winding is possible around the aluminum mandrel or not.

The mixture of the epoxy system was prepared by using resin (Araldite™ MY740) and curing agent (Araldur™ MY918) by 100:85. Liquids were mixed up to homogenous mixing level. Accelerator (DY062) was added into the mixture by 100:1. Epoxy resin, hardener and accelerator was used 1000 g, 850g and 10g, respectively. Whole epoxy system was mixed into the polypropylene beaker by using mechanical stirring. After the mixing process, mixture was not put into the resin bath directly for dispersion of air bubbles to prevent loss of mechanical properties. Fibers were stretched by using tensioner which applied force to the fiber roving. Fibers were impregnated in a resin bath. Paint roller was assembled onto the resin bath to improve resin impregnation of the fibers. Photo of the resin bath is shown in Figure 3.3.



Figure 3.3. Photo of resin bath during the manufacturing of glass fiber reinforced composite tube

Impregnated fibers were wound on a rotating aluminum mandrel with a winding angle of  $\pm 55^\circ$ . Figure 3.4. and Figure 3.5. demonstrate filament winding process. There are three numbers in the picture of filament winding process of hybrid composite tube. The numbers correspond aluminum mandrel, teflon sheet and resin impregnated fibers, respectively in Figure 3.4.



Figure 3.4. Filament winding process of hybrid composite tube

Teflon sheet was covered on cylindrical aluminum mandrel which has 60 mm diameter, 2.5 mm thickness and 130 mm length before winding process. Aluminum mandrel was utilized as a mold in the winding process. Teflon has an important task in this process as a separator between composite tube and aluminum mandrel.



Figure 3.5. Filament winding process of fully glass composite tube

After the filament winding process, composite tubes were cured in an exclusive oven at 80 °C for 2 hours and at 120 °C for 2 hours as shown in Figure 3.6. During the curing process, wet fiber wound composite structure rotates with constant velocity to prevent aggregation of epoxy resin. After the curing process, composite tube was ejected from aluminum mandrel.



Figure 3.6. Specialized curing oven for filament winding

Totally, six various types of fiber reinforced cylindrical composite structure were manufactured in this thesis. Manufactured composite tubes can be seen in Figure 3.7.

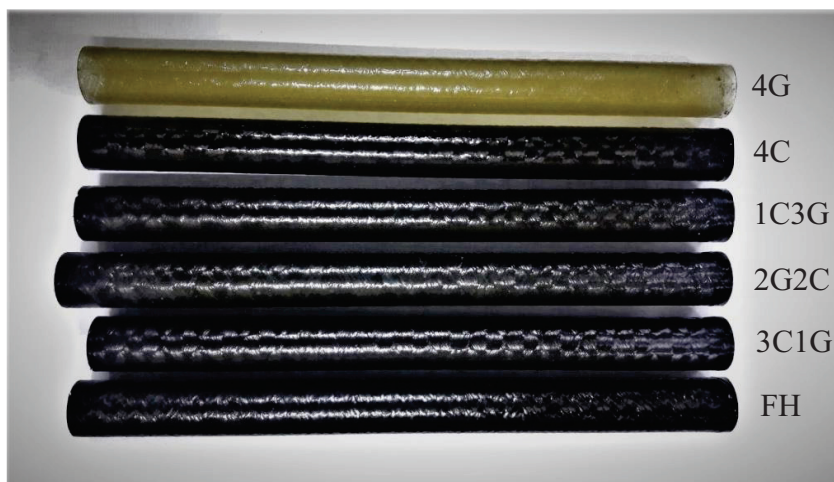


Figure 3.7. Manufactured composite tubes by using filament winding technique (G: glass, C: carbon, FH: filament hybrid)

Only glass fiber and only carbon fiber were wound on aluminum mandrel, they are the first and second produced tubes, respectively. For the third, fourth and fifth produced tubes, glass fiber and carbon fiber with different stacking sequences were wrapped on rotating mandrel to get hybrid filament wound tubes. Last produced tube is known as a filament hybrid, in this winding process simultaneously two different fiber types were wet wound on rotating mandrel. Carbon fiber as well as glass fiber was applied to each layer. In the first column of the Table 3.2. layer configurations of each produced tubes are given. However, shortly defined layers and average thicknesses of whole manufactured tubes are presented respectively in Table 3.2. The short demonstration of layers was utilized throughout the thesis to represent each composite tube.

Table 3.2. Stacking sequences and average thicknesses of each produced structures (G: glass, C: carbon, FH: filament hybrid)

Layers	Short Demonstration of Layers	Average Thickness (mm)
<b>G / G / G / G</b>	<b>4G</b>	2.04
<b>C / C / C / C</b>	<b>4C</b>	1.42
<b>C / G / G / G</b>	<b>1C3G</b>	1.86
<b>C / G / C / G</b>	<b>2G2C</b>	1.79
<b>C / C / C / G</b>	<b>3C1G</b>	1.68
<b>C+G / C+G / C+G / C+G</b>	<b>FH</b>	2.15

The manufactured each composite tube were cut using a diamond saw from two edges to prepare test samples. Every composite tube has 4 layers and 1000 mm length. Schematically representation of composite tube can be seen in Figure 3.8.

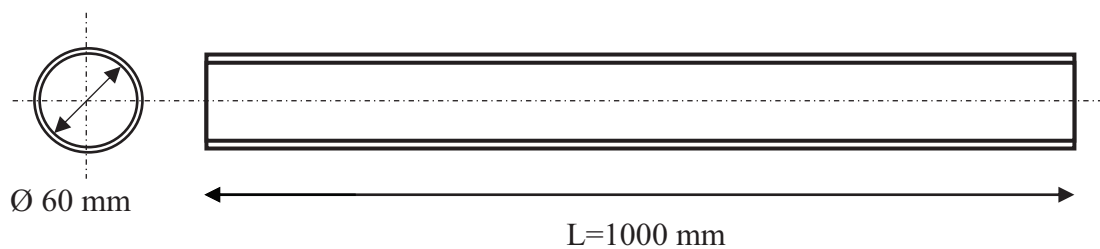


Figure 3.8. Schematically representation of composite tube

In this experimental study, the investigation of the effect of fiber orientation of composite pipes on different ply sequence was performed. Additionally, winding angle of fiber reinforced composite pipe was not changed for every specimen and  $\pm 55^\circ$  is one of the constant degrees during the manufacturing of all specimen. The degree was clearly seen as shown in Figure 3.9.

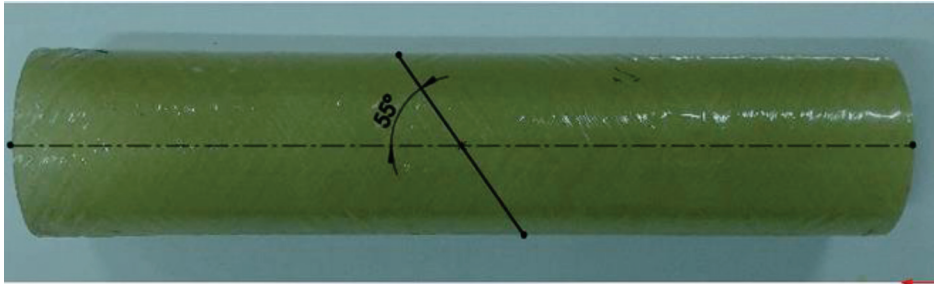


Figure 3. 9.  $55^\circ$  winding angle of wound composite tube

### 3.4. Mechanical Testing of Composite Tubes

In this study, mechanical properties of filament wound composite tubes were investigated according to ASTM standard. Two mechanical tests such as apparent hoop tensile test and radial compression test were carried out.

#### 3.4.1. Apparent Hoop Tensile Test

The apparent hoop tensile test by split disc method was performed onto filament wound cylindrical composite structures in order to obtain apparent hoop tensile strength. The apparent hoop tensile test was applied according to ASTM D2290 Procedure A (ASTM D2290 - 2003). Shimadzu™ AG-IC Series test machine with a maximum capacity of 100 kN was utilized for apparent hoop tensile test by using specialized split disk test apparatus. The schematic representation of the test apparatus is shown in Figure 3.10.

At least 3 specimens for each filament wound composite structure group were prepared with a 4 axis CNC machine. Excess ends of the composite tubes were cut with



a diamond saw. After the cutting process, composite tubes were drilled by using a 4 axis CNC machine with drill head. The drilling process was carried out step by step because of delicate layers of composite tubes. Three different drill head was used with different diameter as 4 mm, 8 mm and 10 mm, respectively to prevent delamination between inter and intra layers of composite tubes. Ring specimens were sectioned from drilled composite tubes by using diamond saw.

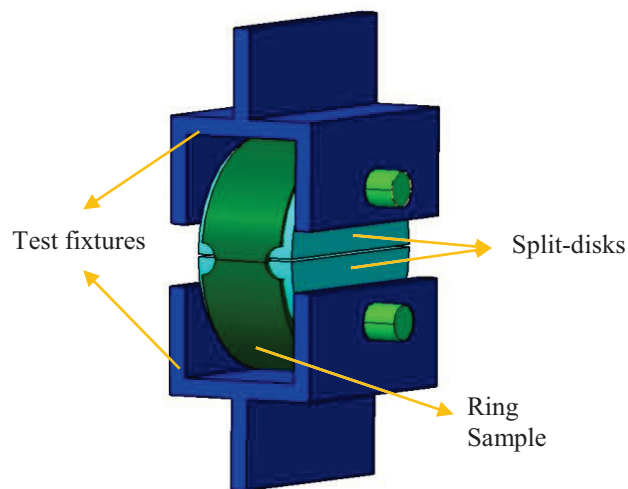


Figure 3. 10. Schematic representation of split disk test setup

The faces and reduced areas of the test specimens were abraded in order to obtain soft surfaces. Dimensions of ring test specimens and sectioned rings are shown in Figure 3.11.

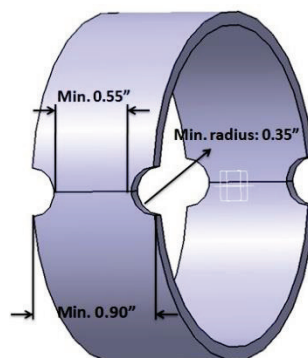


Figure 3.11. Dimensions of ring test specimens (Source: ASTM D2290-00 2003)

Load and displacement data were recorded and taken from the machine until the break point of the specimen. Data were used for calculation of the apparent hoop tensile strength. Determination of the apparent hoop tensile strength of the ring specimens was measured by using the following Equation 3.1:

$$\sigma_{hts} = \frac{F_{max}}{(2A_{min})} \quad (3.1)$$

Where  $F_{max}$  is the maximum force up to failure and  $A_{min}$  is the minimum cross – sectional area and represents ultimate hoop tensile strength. The whole of the prepared test specimens was tested with a constant cross-head speed of machine that was set to 5 mm/min. All test specimens prepared according to the standard ASTM D2290 can be seen in Figure 3.12.

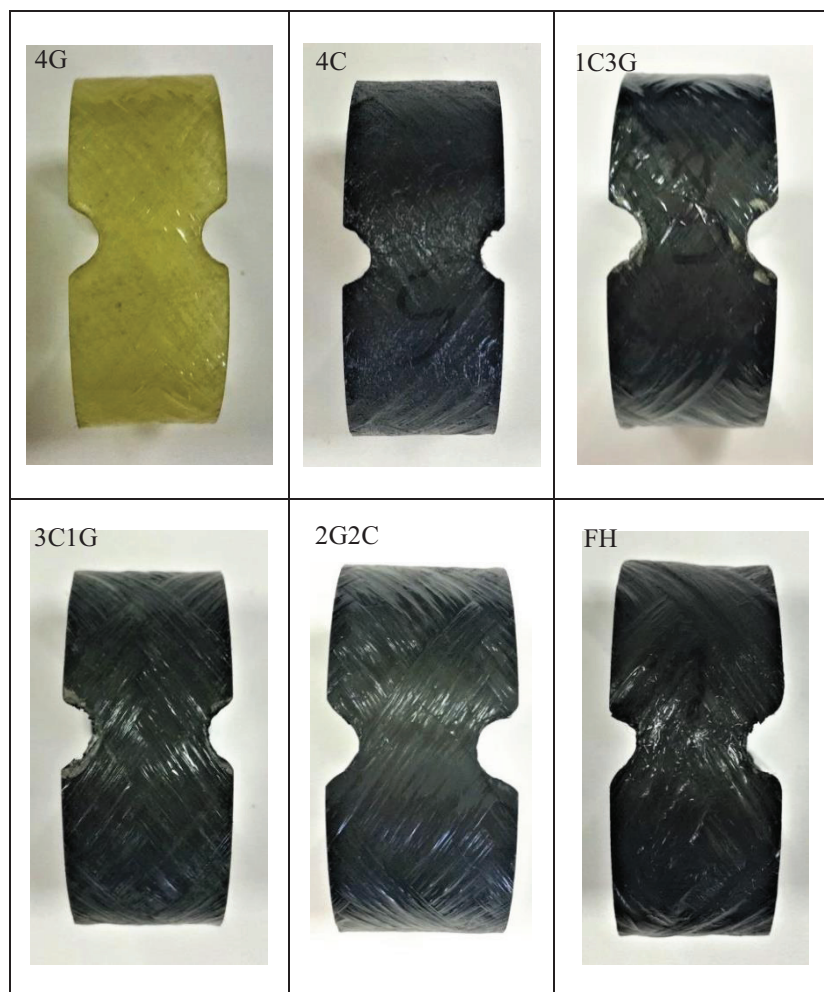


Figure 3.12. Sectioned filament wound ring specimens before apparent hoop tensile test

The ring specimens were placed onto the split disk test apparatus which was assembled on the tensile test fixture as shown in Figure 3.13.

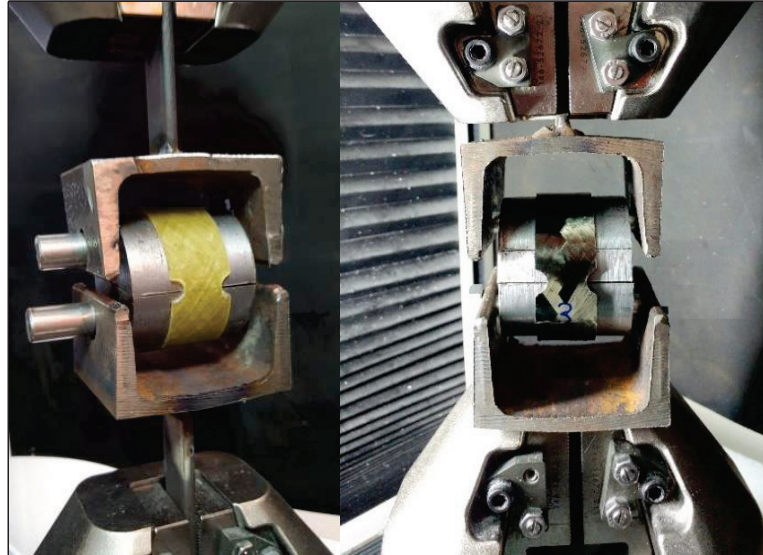


Figure 3.13. Composite ring specimens were inserted split disks for apparent hoop tensile test

### 3.4.2. Radial Compression Test

Radial compression test method is generally used to obtain stiffness of composite materials according to ASTM D2412 (ASTM D2412 Standard 2009). Universal test machine (Shimadzu AG-IC 100 kN) with compression apparatus were used for radial compression test at room temperature. Schematic representation of radial compression test setup can be seen in Figure 3.14.

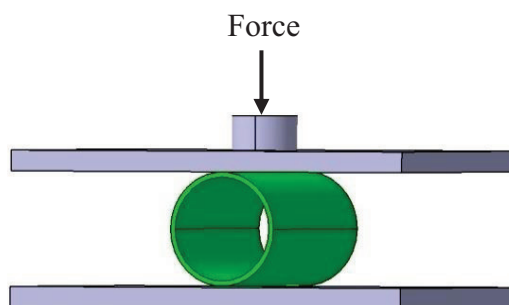


Figure 3.14. Schematic representation of test setup

The radial compression test was utilized to observe pipe stiffness strength and percentage of deflection values of the composite pipes. Specimens were cut from the produced cylindrical composite tube. All the test specimens were prepared with the same dimensions and cut with diamond blade after that radial compression test specimens were obtained with 180 mm in length and 60 mm in inner diameter.

Composite test specimens were placed between upper and lower apparatus which are rectangular shaped composite platforms. Photograph of radial compression test setup can be seen in Figure 3.15. Compression force was applied in radial direction and through composite pipe until failure occurred. Cross-head speed of universal test machine was fixed 12.5 mm/min depends on the ASTM standard. At least 3 specimens for each group were tested and deflection (mm) and force (N) data were recorded.

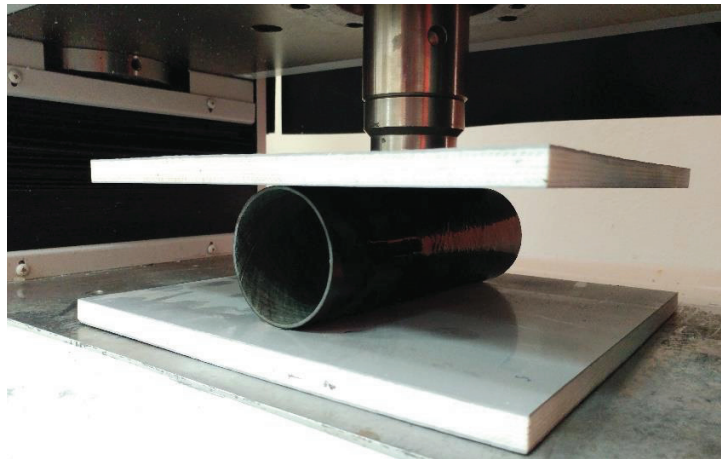


Figure 3.15. Test setup of radial compression test

Calculation of stiffness (PS) and percent of deflection (PD) of the composite pipe specimens were obtained according to Equation 3.2 and Equation 3.3, respectively;

$$PS = (F/\Delta y) \quad (3.2)$$

where F is the applied load at which crack occurred in Newton, and  $\Delta y$  is the % 5 deflection of the inner diameter of the samples.

PD is the percent of deflection and d is the internal diameter of the sample in millimeter. In Equation 3.3  $\Delta y$  is the total deflection where the failure occurred.

$$PD = \Delta y / d \quad (3.3)$$

At least three composite pipe specimens for each set were tested and force-deflection data were recorded. Example images of each test specimen before testing are shown in Figure 3.16.

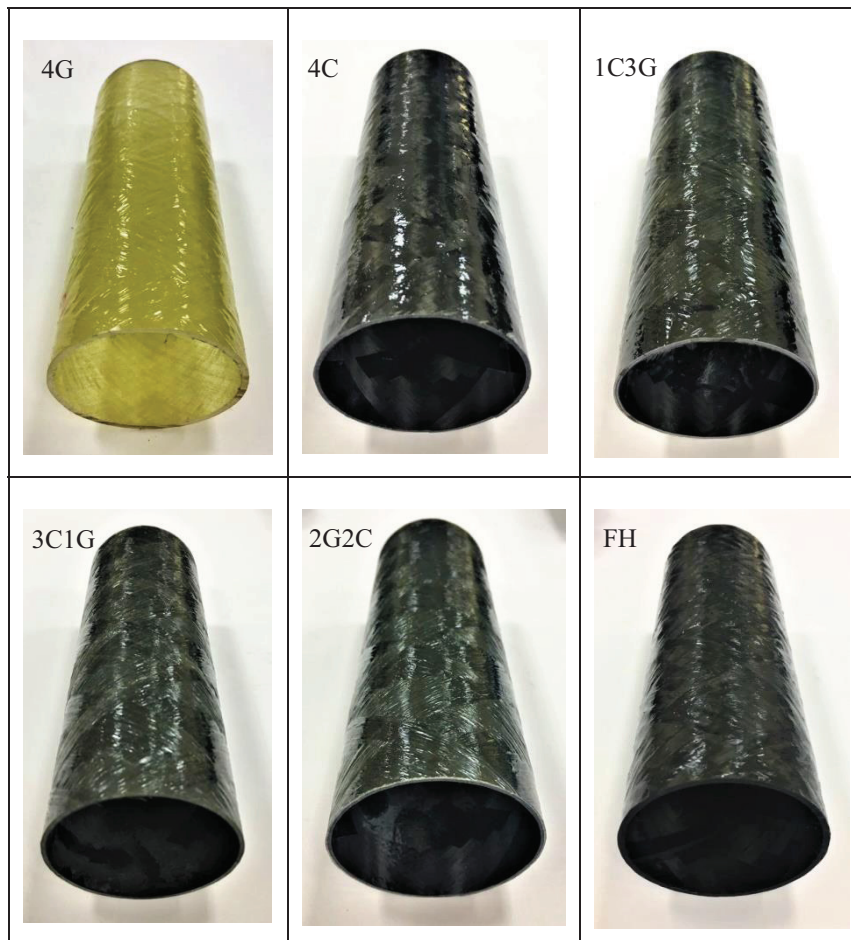


Figure 3.16. Radial test specimens which are sectioned from filament wound composite structures

### 3.5. Calculation of Fiber Mass Fraction

The fiber mass fraction of composite pipes was measured by using matrix digestion test. The test was carried out according to ASTM D3171 (2000) standard. Procedure B is an ideal method to separate fiber and matrix constituents. The procedure consists of two components that are sulfuric acid ( $H_2SO_4$ ), and hydrogen peroxide ( $H_2O_2$ ).

In this test, two composite specimens from each group were prepared before the digestion test. At least two test specimens from each composite tube were sectioned by using a diamond cutter. Glass beakers have a minimum 100 ml volume to prevent bubbling over. Composite specimen with 2 g weight was located into a glass beaker. Minimum 20 ml sulfuric acid was put onto a specimen by using a pipette. Beaker was placed above a preheated plate. When the solution became dark, approximately 35 ml hydrogen peroxide was added step by step. This section of the digestion test is very important for human health. Precautions were taken before digestion. Each drop of hydrogen peroxide was caused to splash and dark fume. Peroxide was applied until the solution was seemed clear and floating fibers appeared above the solution. Floating fibers washed with distilled water and dried in an oven at 100 °C for 1 hour. After drying, each specimen was weighed.

$$W_r = (M_f / M_i) \times 100 \quad (3.4)$$

Equation of weight percent of fiber content is shown in Equation 3.4.  $W_r$ ,  $M_i$ , and  $M_f$  represents weight percent, initial mass of the sample, and final mass of the sample, respectively. The fiber weight fraction of composite specimens was calculated with this equation.

### **3.6. Manufacturing of Composite Plates**

Glass and carbon fiber wounded plates were produced with filament winding technique. Fiber wound composite plates was manufactured by using glass and carbon fiber and epoxy resin system to obtain mechanical properties of used materials. Rectangular shaped aluminum plate which has 25 mm thickness, 300 mm wide and 400 mm length was used as mold that it is connected cnc chuck by short mandrel. The aluminum plate is rotated with the chuck of cnc and fiber carriage is moved throughout horizontal axis and stayed next to the aluminum plate.

Teflon film was laid down on the surrounding of plate as shown in Figure 3.17 due to separator effect of teflon before manufacturing process started. Teflon film is beneficial for ejecting fiber wound plate from aluminum plate.

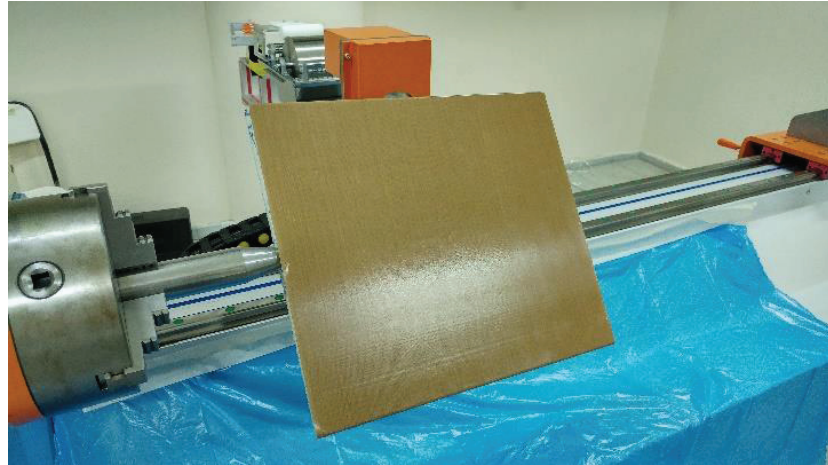


Figure 3.17. Aluminum plate was wound by teflon film

CNC controlled winding machine was utilized for manufacturing of composite plates. Process is similar to composite tube manufacturing method. In this method fiber wound around the aluminum plate with 90 degree. Resin impregnated fibers were wound from one end to other end of pattern and the manufacturing process was continued up to 4 layers as shown in Figure 3.18.

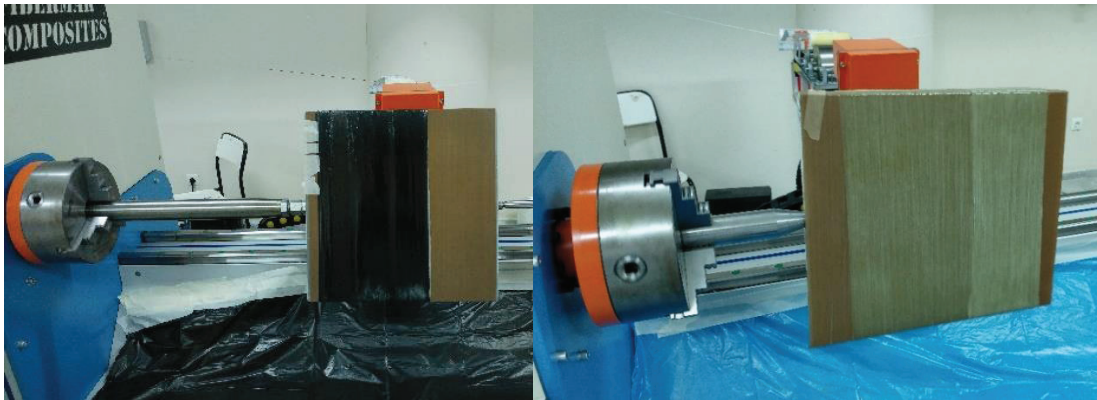


Figure 3.18. Manufacturing of carbon fiber wound plate (a), manufacturing of glass fiber wound plate (b)

Fiber wound plates were cured inside an special designed oven which its mandrel rotates during the curing process according to the data sheet of Araldite™ epoxy system. Aggregation of epoxy resin on fiber wound plate was prevented with this oven. The plates were cured at 80 °C for 2 hours and at 120 °C for 2 hours.

### 3.7. Investigations of Thermal Properties of Composite Plates

In order to observe viscoelastic behavior of filament wound composite plate test specimens which were sectioned according to ASTM standard dynamic mechanical analysis was carried out.

#### 3.7.1. Dynamic Mechanical Analysis

The dynamic mechanical analysis (DMA) is used to exhibit viscoelastic characterization of composite materials. Dynamic mechanical analysis is the preferred method of measurement for glass transition temperature ( $T_g$ ) due to its higher sensitivity compared to other test methods which are DSC and DTA methods.

Dynamic mechanical analysis (DMA) was applied to the composite specimens which were cut from glass and carbon fiber wound plate. The dimensions of composite specimens were 10 mm in width and 60 mm in length. TA Instruments Q800 was utilized as shown in Figure 3.19. Test was occurred in a dual cantilever mode which specimen is clamped at two ends and bended in the mid-point of specimen. Furnace was heated from room temperature to 200 °C with 5 °C/min heating rate. The glass transition temperature of composite specimens was revealed by using tangent delta ( $\tan\delta$ ) peak.

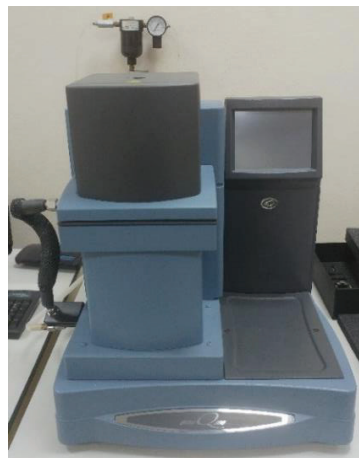


Figure 3.19. DMA testing machine



## CHAPTER 4

### RESULTS AND DISCUSSION

This chapter of the thesis includes results, graphs and photographs of tested filament wound composite specimens. Firstly, fiber content test and dynamic mechanical analysis results are presented. Lastly, mechanical test results as apparent hoop tensile test and radial compression of composite ring specimens and graphical demonstration of that results are given for each group.

#### 4.1. Microstructural Properties of Filament Wound Composite Tubes

##### 4.1.1. Fiber Mass Fraction

Fiber mass fraction is significantly important for composite materials to obtain higher mechanical properties. The fiber content of composite pipes was explored according to ASTM D3171 (2000) standard by using sectioned composite specimens. The test standard was selected for carbon fibers which are not suitable for burn-off test.

Floating fibers during digestion process and glass and carbon fibers together after drying process at 100 °C are shown in Figure 4.1.

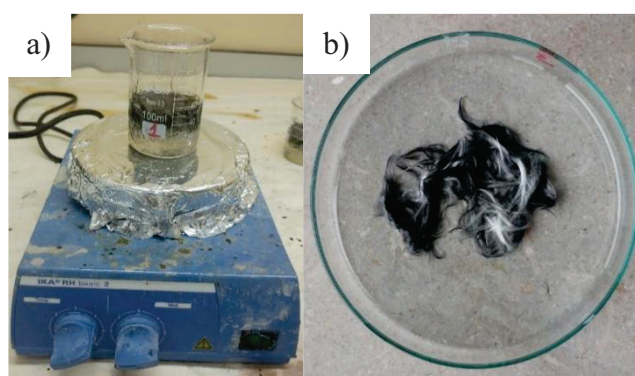


Figure 4.1. Floating carbon fibers after the hydrogen peroxide addition (a), glass fibers and carbon fibers are together after drying (b)

The results of fiber content of manufactured composite cylindrical structures are listed in Table 4.1. Average fiber content was found about approximately 62 wt% by 2.64 standard deviation. Fiber-matrix constituent is significantly important for thickness of manufactured composite tubes, they have a relationship with each other. For this reason, fiber mass ratio was considered during investigation of mechanical properties.

There is difference between wettability level of glass and carbon fiber as seen obviously. Hybrid composite tubes show higher fiber mass ratio due to carbon fiber. As reference values, average fiber content of glass and carbon fiber reinforced composite specimens were measured as 58.14 % and 61.41 %, respectively.

Table 4.1. Average fiber weight ratios of sectioned composite tube specimens

<b>Sample</b>	<b>Avg. Fiber Content (wt. %)</b>
<b>4G</b>	58.14
<b>4C</b>	61.41
<b>1C3G</b>	63.94
<b>3C1G</b>	65.71
<b>2G2C</b>	61.70
<b>FH</b>	63.87

## **4.2. Thermal Properties of Filament Wound Composite Plates**

### **4.2.1. Dynamic Mechanical Analysis Results**

Dynamic mechanical analysis (DMA) was performed according to ASTM D7028 (ASTM D7028 2012). Test was applied onto two different composite structures as glass and carbon fiber wound composite plates to obtain glass transition temperature (T<sub>g</sub>).

Table 4.2. Test results of filament wound composite plate

<b>Sample</b>	<b>Glass Transition Temperature (°C)</b>	<b>Storage Modulus (MPa)</b>
<b>G (4 layers)</b>	154.80	3259.77
<b>C (4 layers)</b>	153.43	5272.18

Results of Tg and storage modulus (E') are shown in Table 4.2. Results of carbon and glass fiber reinforced epoxy composite test specimens demonstrate rather near values. There is no significant difference between reference value and obtained values.

Dynamic mechanical analysis is a very common test method for investigation of viscoelastic behaviors. Glass transition temperature of wound composite tubes is crucial for hot fluid piping systems. Storage and loss modulus, tan delta and temperature values of composite plate specimens are shown with graphs in Figure 4.2 and 4.3.

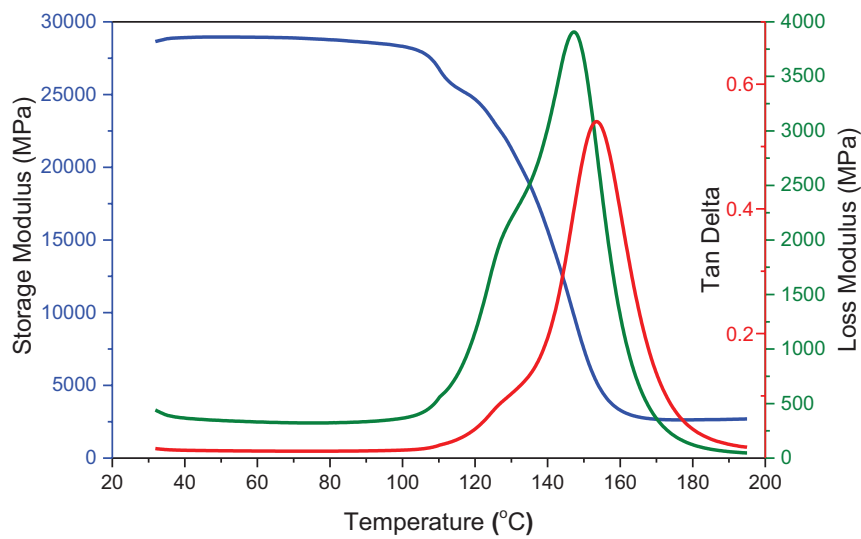


Figure 4.2. Dynamic mechanical analysis result of carbon fiber wound plate specimen

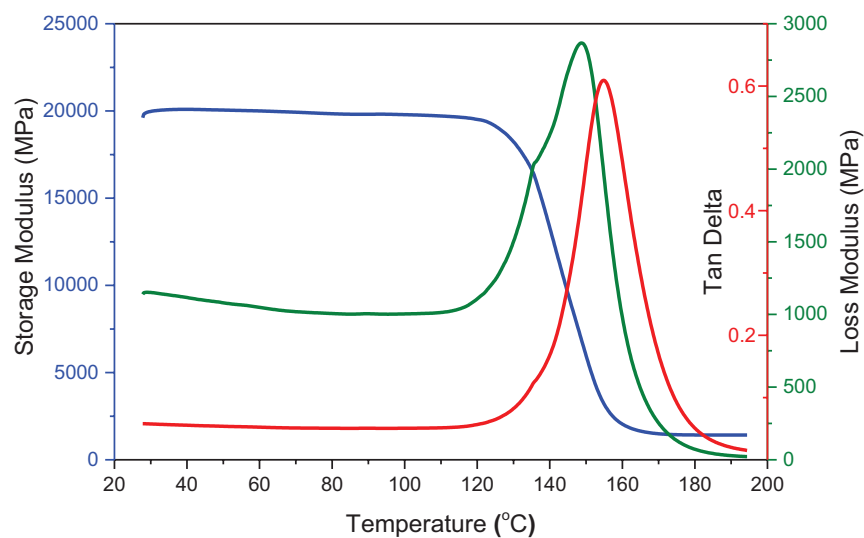


Figure 4.3. Dynamic mechanical analysis result of glass fiber wound plate specimen

### 4.3. Mechanical Properties of Filament Wound Composite Tubes

#### 4.3.1. Apparent Hoop Tensile Test Results

The apparent hoop tensile strength of  $[\pm 55^\circ]_4$  filament wound composite ring specimens was investigated by using a split disk test method. The test results and minimum cross-sectional areas of each specimen are listed through Tables 4.3 to 4.7.

Table 4.3. Tensile properties of G/G/G/G wound ring specimens

Sample	Hoop Tensile Strength (MPa)	$A_{min}$ (mm <sup>2</sup> )
4G - 1	311.07	32.56
4G - 2	293.82	31.47
4G - 3	322.78	32.24
<b>Average</b>	<b>309.22</b>	<b>32.09</b>
<b>St. Dev. (<math>\pm</math>)</b>	<b>14.5</b>	<b>0.5</b>

Table 4.4. Tensile properties of C/C/C/C wound ring specimens

Sample	Hoop Tensile Strength (MPa)	$A_{min}$ (mm <sup>2</sup> )
4C - 1	530.81	22.91
4C - 2	501.28	22.40
4C - 3	498.72	22.68
<b>Average</b>	<b>510.27</b>	<b>22.66</b>
<b>St. Dev. (<math>\pm</math>)</b>	<b>17.8</b>	<b>0.2</b>

Table 4.5. Tensile properties of C/G/G/G wound ring specimens

Sample	Hoop Tensile Strength (MPa)	$A_{min}$ (mm <sup>2</sup> )
1C3G - 1	355.36	31.29
1C3G - 2	310.53	28.67
1C3G - 3	323.67	28.17
<b>Average</b>	<b>329.85</b>	<b>29.38</b>
<b>St. Dev. (<math>\pm</math>)</b>	<b>23.0</b>	<b>1.6</b>

Table 4.6. Tensile properties of C/G/C/G wound ring specimens

Sample	Hoop Tensile Strength (MPa)	A <sub>min</sub> (mm <sup>2</sup> )
<b>2G2C - 1</b>	396.39	27.66
<b>2G2C - 2</b>	405.36	26.16
<b>2G2C - 3</b>	377.53	28.45
<b>Average</b>	<b>393.09</b>	<b>27.42</b>
<b>St. Dev. (±)</b>	<b>14.2</b>	<b>1.1</b>

Table 4.7. Tensile properties of C/C/C/G wound ring specimens

Sample	Hoop Tensile Strength (MPa)	A <sub>min</sub> (mm <sup>2</sup> )
<b>3C1G - 1</b>	365.48	25.43
<b>3C1G - 2</b>	399.18	27.65
<b>3C1G - 3</b>	385.16	25.35
<b>Average</b>	<b>383.28</b>	<b>26.15</b>
<b>St. Dev. (±)</b>	<b>16.9</b>	<b>1.3</b>

Table 4.8. Tensile properties of Filament Hybrid (FH) wound ring specimens

Sample	Hoop Tensile Strength (MPa)	A <sub>min</sub> (mm <sup>2</sup> )
<b>FH - 1</b>	432.69	35.47
<b>FH - 2</b>	392.64	32.81
<b>FH - 3</b>	394.05	33.05
<b>Average</b>	<b>406.46</b>	<b>33.78</b>
<b>St. Dev. (±)</b>	<b>22.7</b>	<b>1.4</b>

Calculation of the apparent hoop tensile strength of the ring specimens was measured by using Equation 3.1. according to ASTM D2290. Load and displacement data were recorded and taken from the test machine during the tensile test. Force-displacement graphs of whole ring specimen are shown in Figure 4.4 to 4.9. Linear force-displacement curves are clearly seen in the graph until the failure point.

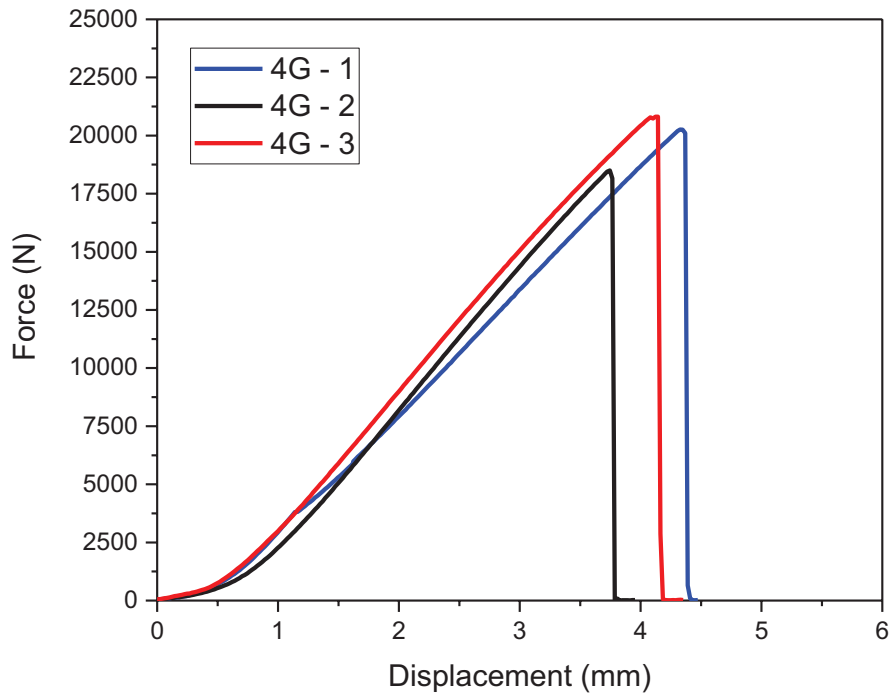


Figure 4.4. Force-displacement curves of G/G/G/G wound composite ring specimens during split disk test

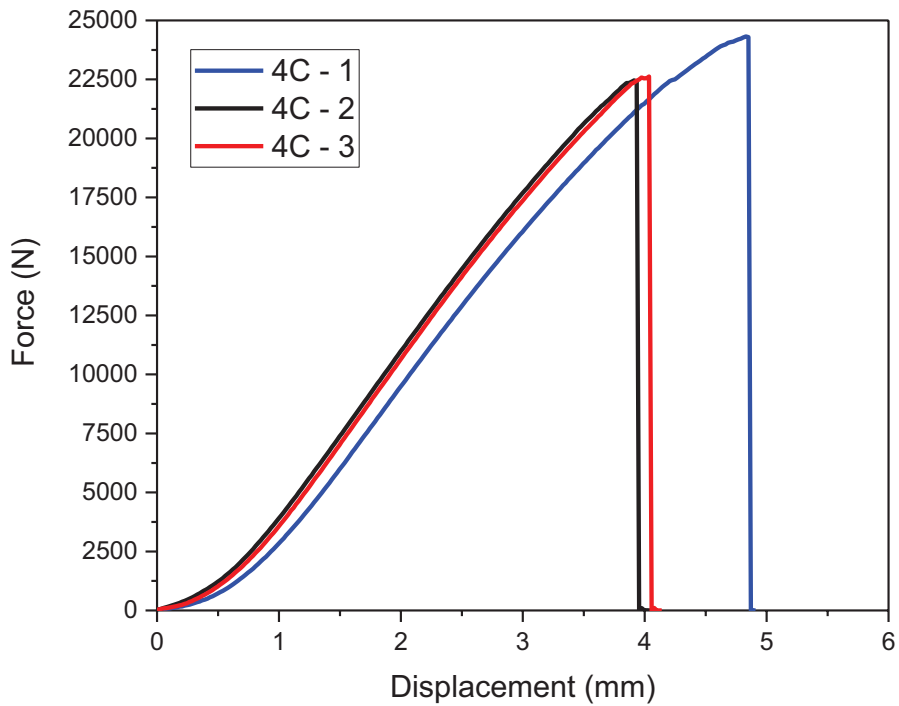


Figure 4.5. Force-displacement curves of C/C/C/C wound composite ring specimens during split disk test

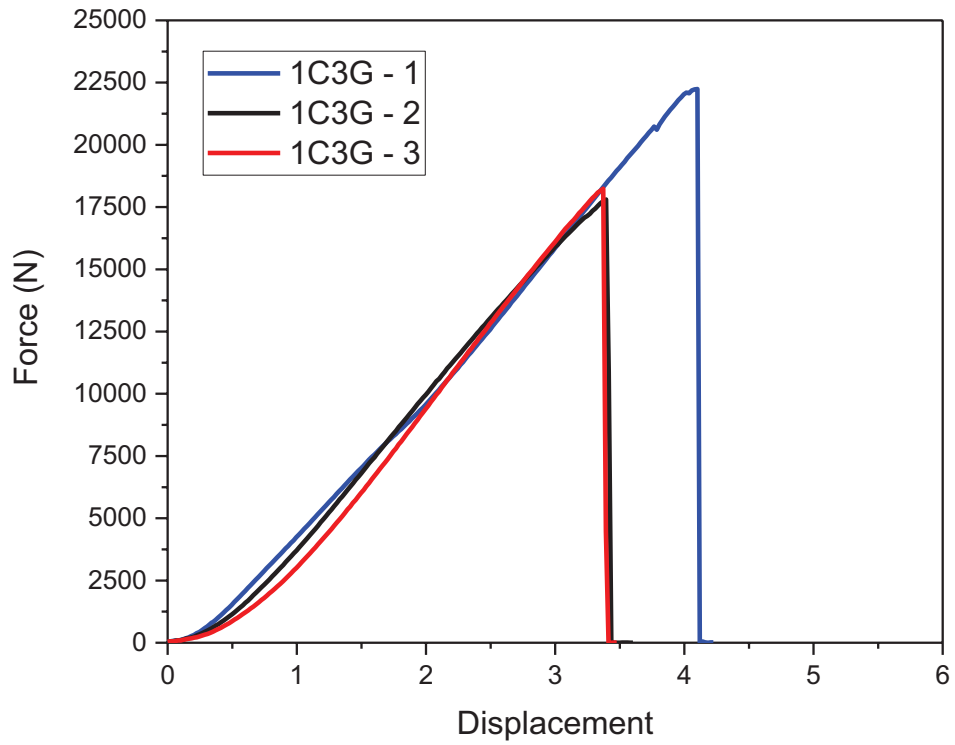


Figure 4.6. Force-displacement curves of C/G/G/G wound composite ring specimens during split disk test

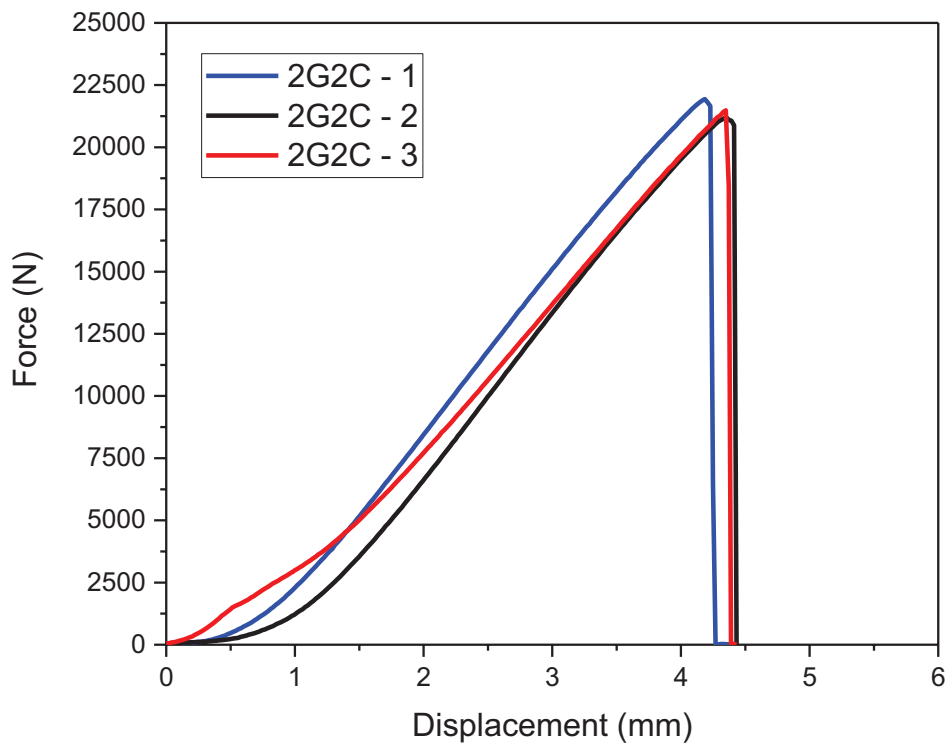


Figure 4.7. Force-displacement curves of C/G/C/G wound composite ring specimens during split disk test

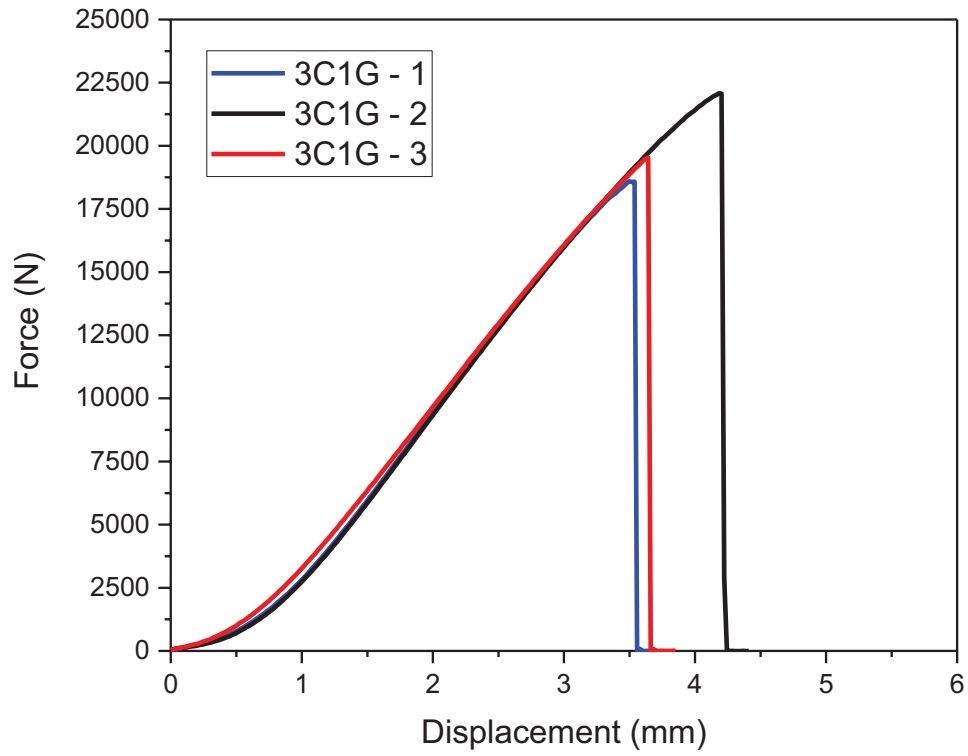


Figure 4.8. Force-displacement curves of C/C/C/G wound composite ring specimens during split disk test

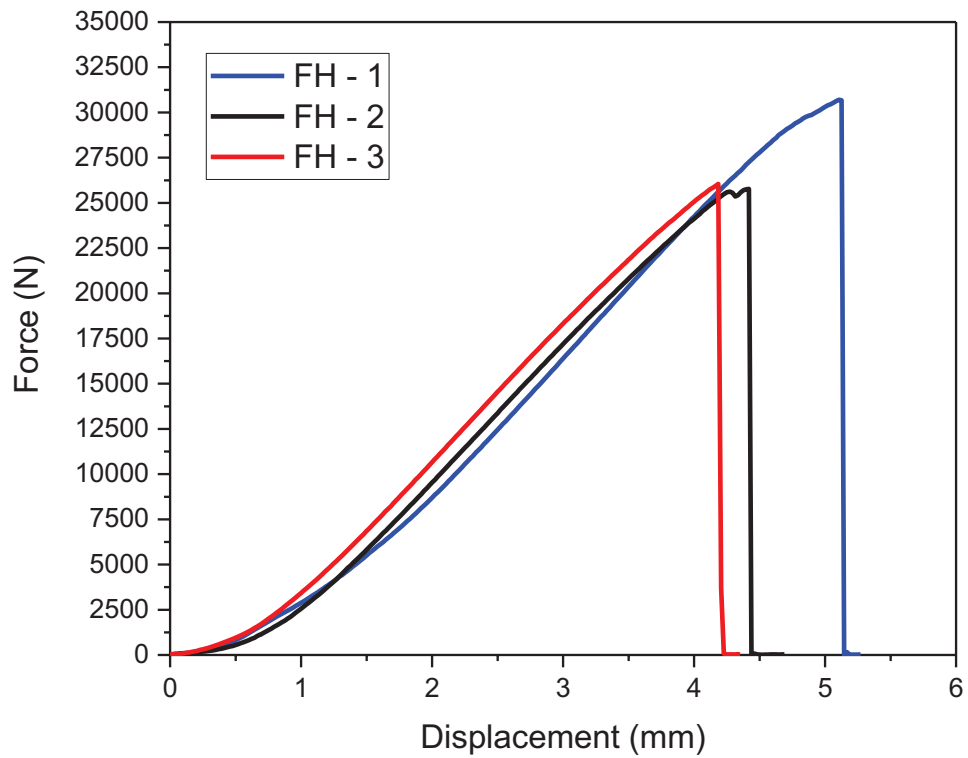


Figure 4.9. Force-displacement curves of glass-carbon Filament Hybrid (FH) wound composite ring specimens during split disk test



The average apparent hoop tensile strength of the  $[\pm 55]_4$  filament wound cylindrical composite structures were measured and given in Table 4.9. As reference values, average apparent hoop tensile strength of glass and carbon fiber reinforced composites were measured as  $309.22 \pm 14.5$  MPa and  $510.27 \pm 17.8$  MPa, respectively. According to study of Srebrenkoska et. al. hoop tensile strength results of the glass fiber reinforced composite tubes show 275 MPa and 285 MPa values for  $\pm 45^\circ$ . Optimum winding angle which is  $55^\circ$  performed higher strength which is listed in Table 4.9.

Table 4.9. Average apparent hoop tensile strength values of composite ring structures

<b>Sample</b>	<b>Average Hoop Tensile Strength (MPa)</b>
<b>4G</b>	$309.22 \pm 14.5$
<b>4C</b>	$510.27 \pm 17.8$
<b>1C3G</b>	$329.85 \pm 23.0$
<b>2G2C</b>	$393.09 \pm 14.2$
<b>3C1G</b>	$404.30 \pm 22.2$
<b>FH</b>	$406.46 \pm 22.7$

As shown in Table 4.9., carbon fiber reinforced pipes exhibited the highest apparent hoop tensile strength as compared to those manufactured with other configuration of fibers, as expected. Moreover, the strength values of the glass fiber reinforced composites were found to be improved by hybridization with carbon fibers.

Incorporation of a single layer of carbon fiber did not have a significant effect on the strength values that increased only 6.67 % while having higher numbers of carbon layers (two and three layers of carbon) significantly improved the strength of glass fiber reinforced structure 27.13 % and 30.76 %, respectively. Sample FH (having commingled hybrid fibers) increased the strength by 31.43 % and showed the highest strength values among the other types of the hybrid composites.

Figure 4.10. represents the failure modes of all the samples after the split disk test. All specimens showed almost similar failure modes.

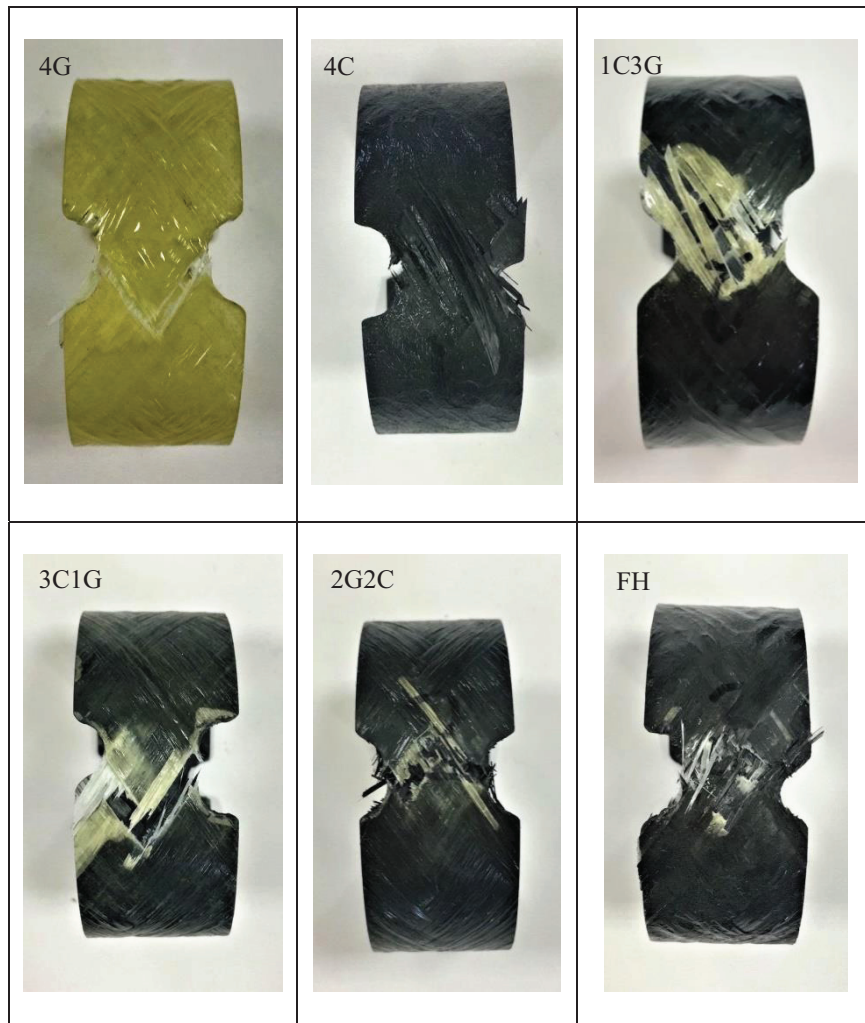


Figure 4.10. Failure modes of the specimens after apparent hoop tensile strength test

When failure mechanism of filament wound composite tubes was observed, the crack started to initiate from one edge of the reduced area of the samples and propagated along the winding path of the fibers. Srebrenkoska et.al. (Srebrenkoska, Risteska, and Mijajlovikj 2015) studied on mechanical properties of glass fiber epoxy composite tubes. Results of this study demonstrate that failure occurs along the line of angles on which fibers are oriented.

#### 4.3.2. Radial Compression Test Results

Radial compression tests were applied to three specimens from each filament wound composite structures which have different stacking sequences. Stiffness and

percentage of deflection values were investigated by changing the position of carbon and glass fiber layers according to ASTM D2412. Radial compression test results of each composite cylindrical structures are listed through Tables 4.10 to 4.15.

Table 4.10. Compressive properties of G/G/G/G wound composite tubes

Sample	Pipe Stiffness (N/mm)	Percentage of Deflection (%)
<b>4G - 1</b>	423.46	50.96
<b>4G - 2</b>	411.16	51.80
<b>4G - 3</b>	433.74	52.36
<b>Average</b>	<b>422.78</b>	<b>51.70</b>
<b>St. Dev. (<math>\pm</math>)</b>	<b>11.30</b>	<b>0.70</b>

Table 4.11. Compressive properties of C/C/C/C wound composite tubes

Sample	Pipe Stiffness (N/mm)	Percentage of Deflection (%)
<b>4C - 1</b>	370.01	13.75
<b>4C - 2</b>	391.40	19.32
<b>4C - 3</b>	372.81	17.03
<b>Average</b>	<b>378.07</b>	<b>16.70</b>
<b>St. Dev. (<math>\pm</math>)</b>	<b>11.62</b>	<b>2.79</b>

Table 4.12. Compressive properties of C/G/G/G wound composite tubes

Sample	Pipe Stiffness (N/mm)	Percentage of Deflection (%)
<b>1C3G - 1</b>	491.23	31.03
<b>1C3G - 2</b>	500.41	23.14
<b>1C3G - 3</b>	473.70	25.13
<b>Average</b>	<b>488.45</b>	<b>26.44</b>
<b>St. Dev. (<math>\pm</math>)</b>	<b>13.57</b>	<b>4.10</b>

Table 4.13. Compressive properties of C/G/C/G wound composite tubes

Sample	Pipe Stiffness (N/mm)	Percentage of Deflection (%)
<b>2G2C - 1</b>	432.71	20.58
<b>2G2C - 2</b>	462.05	22.60
<b>2G2C - 3</b>	457.16	25.20
<b>Average</b>	<b>450.64</b>	<b>22.79</b>
<b>St. Dev. (±)</b>	<b>15.72</b>	<b>2.31</b>

Table 4.14. Compressive properties of C/C/C/G wound composite tubes

Sample	Pipe Stiffness (N/mm)	Percentage of Deflection (%)
<b>3C1G - 1</b>	367.22	20.92
<b>3C1G - 2</b>	371.53	25.00
<b>3C1G - 3</b>	372.20	23.37
<b>Average</b>	<b>370.32</b>	<b>23.10</b>
<b>St. Dev. (±)</b>	<b>2.70</b>	<b>2.05</b>

Table 4.15. Compressive properties of glass-carbon Filament Hybrid (FH) wound composite tubes

Sample	Pipe Stiffness (N/mm)	Percentage of Deflection (%)
<b>FH - 1</b>	678.67	23.08
<b>FH - 2</b>	697.65	19.47
<b>FH - 3</b>	697.31	18.04
<b>Average</b>	<b>691.21</b>	<b>20.19</b>
<b>St. Dev. (±)</b>	<b>10.86</b>	<b>2.59</b>

Force-displacement graphs of the whole filament wound composite test samples are shown in Figure 4.11 to 4.16. Linear force-displacement curves are clearly seen in the graph until the failure point.

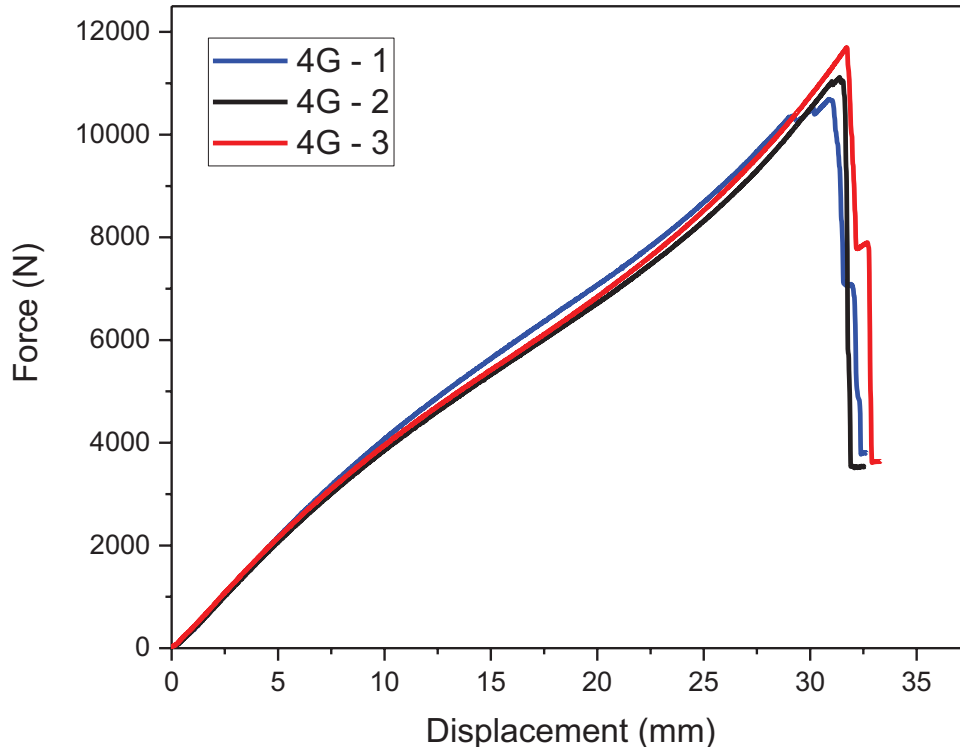


Figure 4.11. Force-displacement curves of G/G/G/G wound composite tubes under radial compression

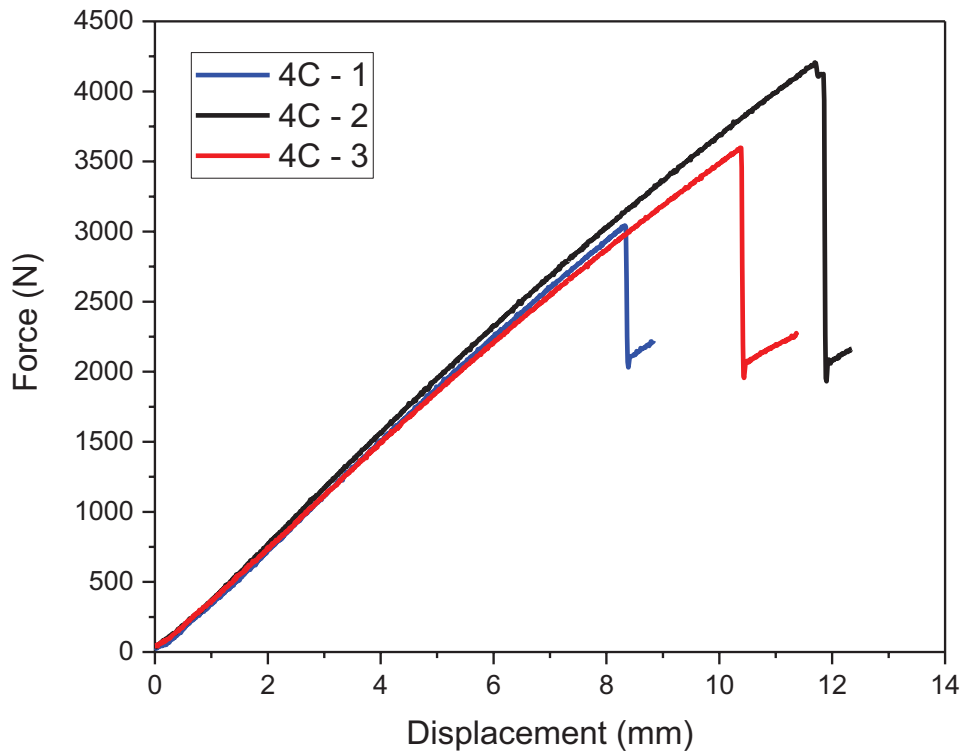


Figure 4.12. Force-displacement curves of C/C/C/C wound composite tubes under radial compression

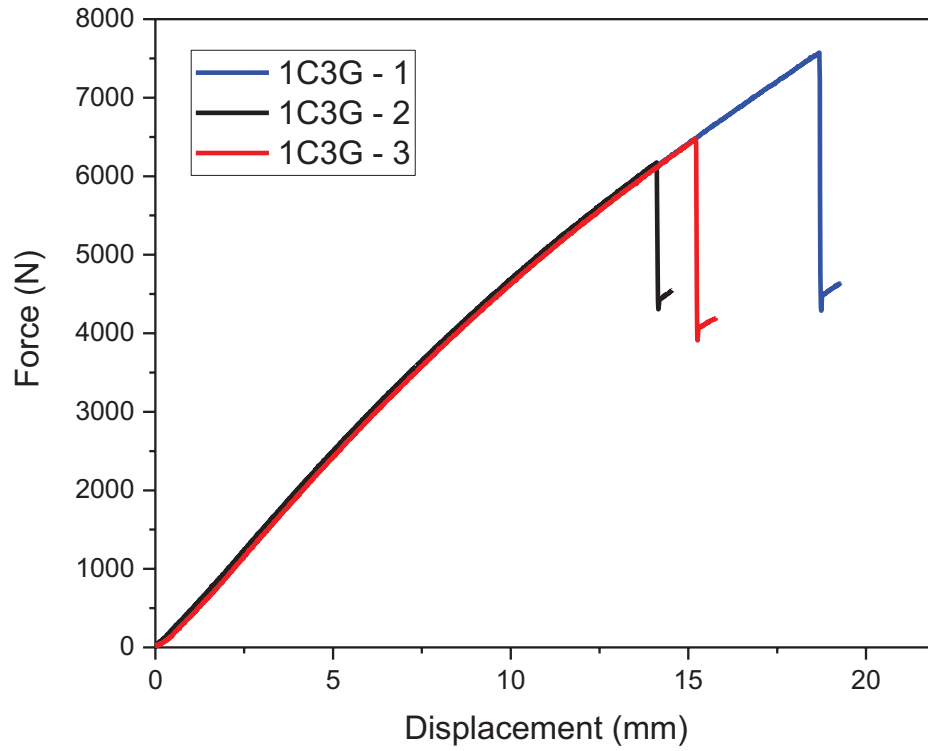


Figure 4.13. Force-displacement curves of C/G/G/G wound composite tubes under radial compression

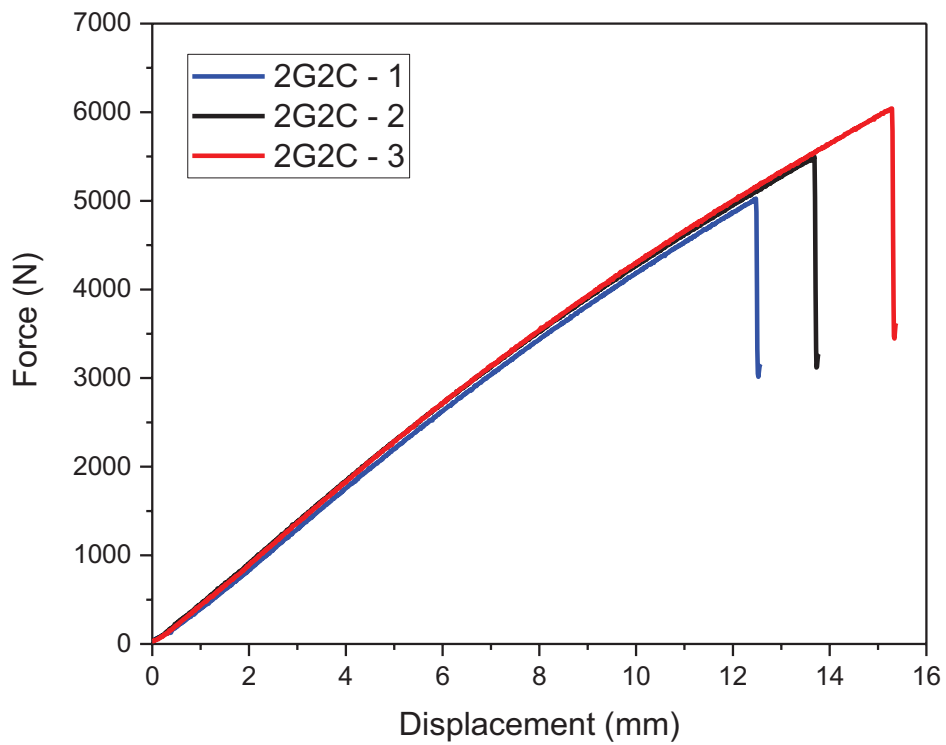


Figure 4.14. Force-displacement curves of C/G/C/G wound composite tubes under radial compression

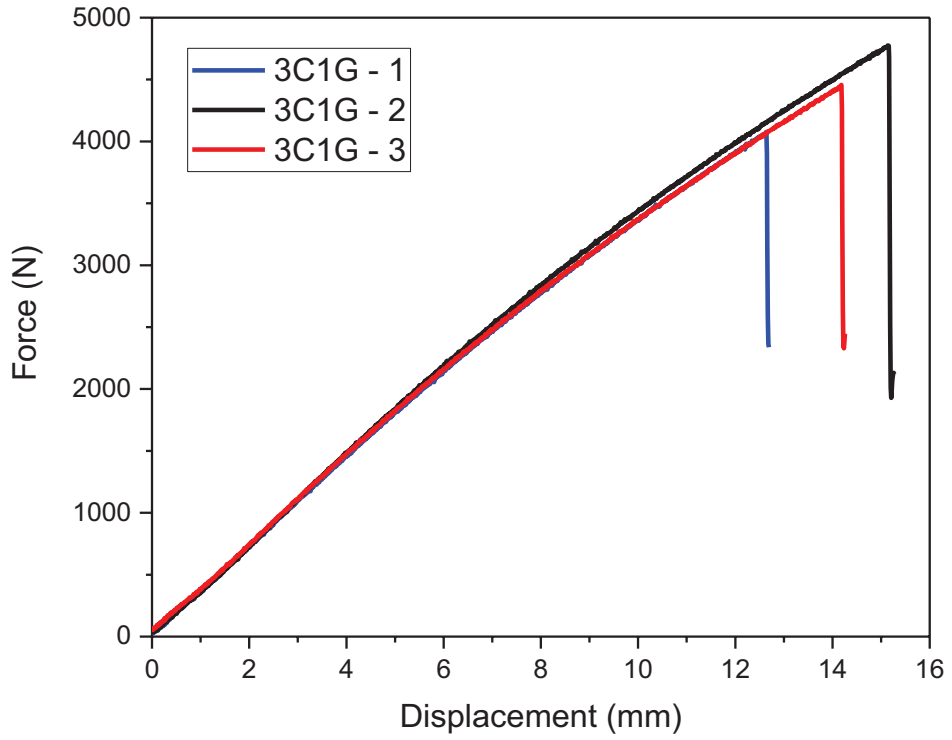


Figure 4.15. Force-displacement curves of C/C/C/G wound composite tubes under radial compression

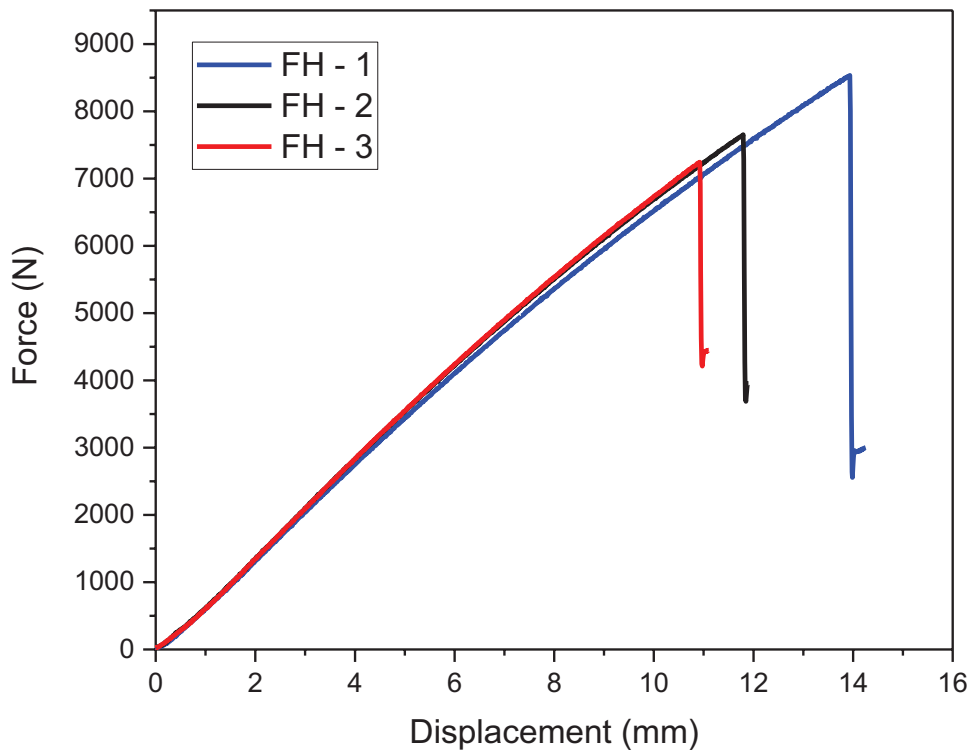


Figure 4.16. Force-displacement curves of glass-carbon Filament Hybrid wound composite tubes under radial compression

Table 4.16 summarizes average stiffness and average percentage of deflection values of the composite samples. The average force-displacement graphs for each sample type obtained during radial compression test are demonstrated in Figure 4.17.

Table 4.16. Average compressive properties of filament hybrid wound composite tubes

Sample	Average Pipe Stiffness (N/mm)	Average Percentage of Deflection (%)
4G	422.78	51.70
4C	378.07	16.70
1C3G	488.45	26.44
2G2C	450.64	22.79
3C1G	370.32	23.10
FH	691.21	20.19

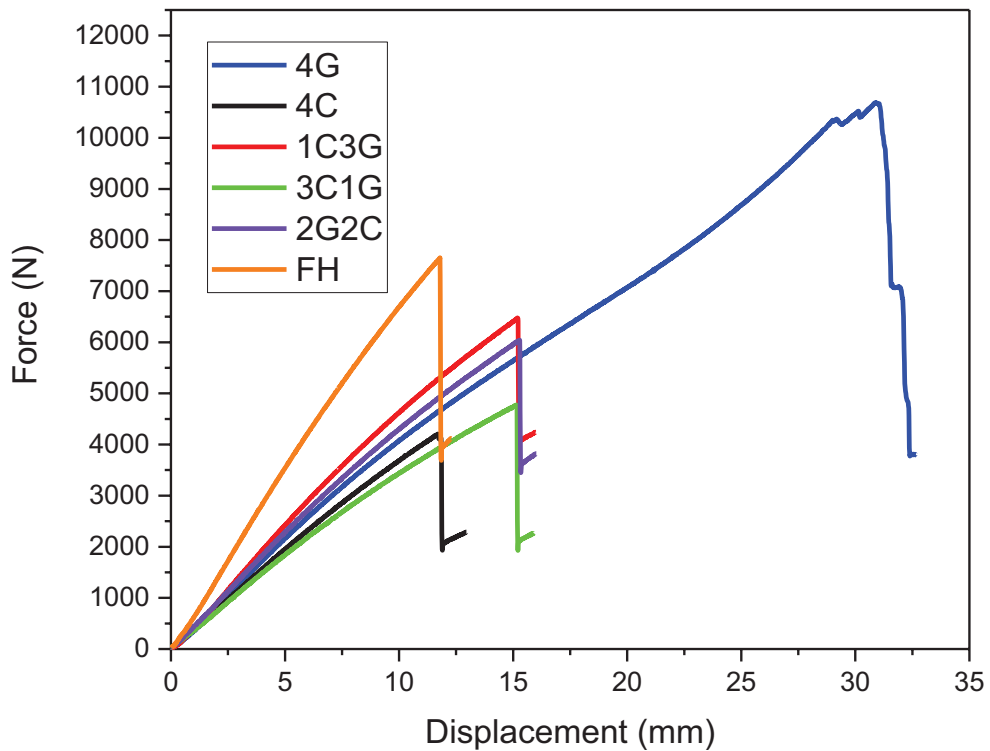


Figure 4.17. Average force-displacement curves of whole produced composite tubes under radial compression



Figure 4.18 demonstrates elliptic form of composite structure under the radial compression.

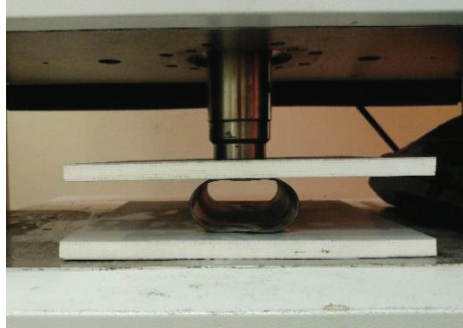


Figure 4.18. Radial compression test specimen under the compression load

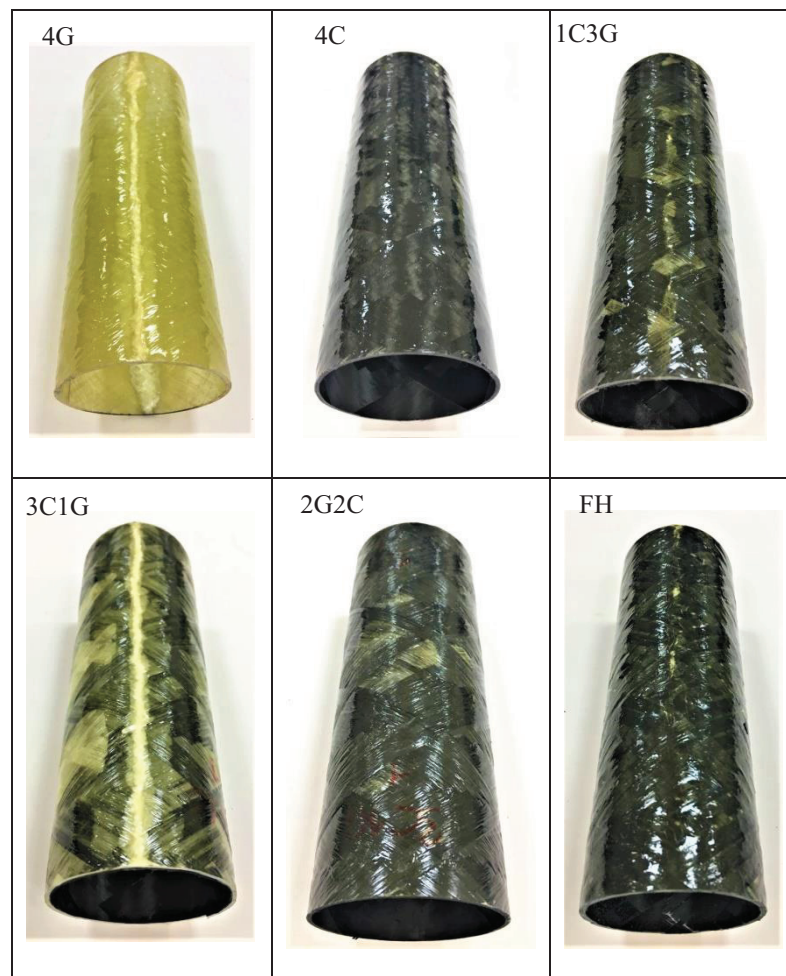


Figure 4.19. Sectioned filament wound composite samples after compression test

The photographs of the specimens after the radial compression test are shown in Figure 4.19. Failure of the composite cylindrical samples occurred as delamination, and they are the same for all the samples.

Stiffness is the resistance against deflection basically, and it is directly proportional to the cubic power of thickness because of the effect of inertia (Rafiee and Habibagahi 2018). Due to this reason thickness has a higher effect on stiffness properties of cylindrical structures than the type of fiber. Therefore, glass fiber reinforced cylindrical structures showed higher stiffness than carbon fiber reinforced structures since they are thicker.

On the other hand, based on the results given in Table 4.16., it is seen that stiffness of glass fiber reinforced composite cylindrical structures were increased by incorporation of carbon fibers, in other words, resistance against deflection was increased. That is also verified by the percent of deflection results. As it is represented, percent of deflection of the cylindrical composite structures was decreased by hybridization. Carbon and commingled fiber reinforced cylindrical structures have the lowest percent of deflection values which are 16.7 % and 20.19 %, respectively. As compared to those other hybrids reinforced cylindrical composite structures, commingled hybrid composite structures have the highest stiffness (691.21 N/mm) and lower deflection percentage (20.19 %) values.

## CHAPTER 5

### CONCLUSIONS

In recent years, polymer composite structures have been utilized in many application areas such as marine, aerospace and lightweight airplanes. Demand of composite structure is increasing day by day depends on the cost-efficiency purpose and improved strength requirements. Moreover, the usage of hybrid fiber reinforced composite structures is significantly important. Hybrid fibers ensure more than one advantages as cost-effective aspect and versatile utilization area for piping, carriage and storage systems.

The primary objective of this study is to development of cylindrical composite structures for applications which require high specific strength and low weight. In this regard, mechanical behavior of cylindrical composite structures with different types of fibers and orientations was studied. Six different types of cylindrical composite structures with glass and carbon fibers as reinforcement were manufactured with optimum winding angle which is  $\pm 55^\circ$  by using filament winding technique.

Mechanical behavior and thermomechanical behavior of  $[55^\circ]_4$  filament wound composite tubes were investigated to determine their apparent hoop tensile strength, stiffness, percentage of deflection and glass transition temperature.

Apparent hoop tensile strength which represents hydrostatic failure strength was carried out firstly. Carbon fiber and glass fiber reinforced structures were used as a reference, and the results of hybrid reinforced cylindrical structures were compared. Carbon fiber usage slightly improved the hoop tensile strength of composite tubes. Commingled hybrid cylindrical composite structures showed the highest strength among the other hybrid structures. Moreover, it was observed that increased carbon layer in composite tubes demonstrated higher strength value than only glass fiber wound composite tube specimens. According to literature, failure mechanism of apparent hoop tensile test is appropriate. Crack initiated from reduced area and continued throughout the line of winding angle.

Ovality of the composite pipes under the radial compression is caused irregular situation. Irregularity of composite tube directly affect working performance for instance fluid transmission. Stiffness analysis is a fundamental point for piping systems.

Radial compression test results showed that hybridization of composite cylindrical structures decreased the percent deflection of the samples, in other words, resistance of cylindrical structures against deflection increased. Percentage of deflection value of only glass fiber reinforced composite tube was obtained 51.7 %. Based on the results, percentage of deflection of hybrid composite tubes decreased step by step thanks to the addition of carbon fiber layers.

Stiffness of the composite tubes depends on the thickness of the composite structures. Increasing of carbon fiber reinforced ply into the hybrid composite tubes resulted in a decrease of the thickness of tube therefore stiffness values decreased. Filament hybrid composite tubes have the highest stiffness value than the reference value. As seen in the results approx. 65 % increased stiffness value was observed.

According to the results of matrix digestion test, fiber content of each composite tube was similar. It was clearly demonstrated that same fiber tension and optimum resin impregnation were applied to the produced composite tubes. Average fiber content was found about approximately 62 %. Furthermore, the choice of fiber and the text of the fiber determined the fiber content into the composite structure. Dynamic mechanical analysis was also performed. The glass transition temperature of two different composite plate test specimens was obtained. There is no significant variation between two samples.

Consequently, the experimental results show that hybridization of the filaments, increased the strength, decreased the deflection percentage compared to glass fiber reinforced pipes and reduced the cost compared to carbon fiber pipes since less carbon fiber was used. Among the hybrid cylindrical composite structures, commingled hybrid reinforced pipes showed the optimal results.

## REFERENCES

- 2290-00, ASTM D. 2003. "Standard Test Method for Apparent Hoop Tensile Strength of Plastic or Reinforced Plastic Pipe by Split Disk Method." *An American National Standard D 2290-00*: 1–5. <https://doi.org/10.1520/D2290-08.2>.
- Almeida, José Humberto S., Marcelo L. Ribeiro, Volnei Tita, and Sandro C. Amico. 2017. "Damage Modeling for Carbon Fiber/Epoxy Filament Wound Composite Tubes under Radial Compression." *Composite Structures* 160 (January): 204–10. <https://doi.org/10.1016/j.compstruct.2016.10.036>.
- AWWA. 1999. *Fiberglass Pipe Design Manual M45*. <http://arco-hvac.ir/wp-content/uploads/2018/04/AWWA-M45-Fiberglass-Pipe-Design-Manual-1996.pdf>.
- Barsoum, I., and K.F. Al Ali. 2015. "A Procedure to Determine the Tangential True Stress-Strain Behavior of Pipes." *International Journal of Pressure Vessels and Piping* 128 (April): 59–68. <https://doi.org/10.1016/j.ijpvp.2014.11.002>.
- Bezerra, Renato, Frederik Wilhelm, Sebastian Strauß, and Holger Ahlborn. 2015. "Manufacturing of Complex Shape Composite Parts through the Combination of Pull-Braiding and Blow Moulding." *ICCM International Conferences on Composite Materials 2015-July* (July): 19–24.
- D3171, ASTM. 2000. "Standard Test Methods for Constituent Content of Composite Materials" 76 (February).
- D7028, ASTM. 2012. "Standard Test Method for Glass Transition Temperature ( DMA Tg ) of Polymer Matrix Composites by Dynamic Mechanical Analysis ( DMA ) 1" i (C): 1–14. <https://doi.org/10.1520/D7028-07E01.2>.
- Diniz Melo, José Daniel, Flaminio Levy Neto, Gustavo De Araujo Barros, and Fausto Nogueira De Almeida Mesquita. 2011. "Mechanical Behavior of GRP Pressure Pipes with Addition of Quartz Sand Filler." *Journal of Composite Materials* 45 (6):

717–26. <https://doi.org/10.1177/0021998310385593>.

Ellul, Brian, and Duncan Camilleri. 2015. “The Influence of Manufacturing Variances on the Progressive Failure of Filament Wound Cylindrical Pressure Vessels.”

*Composite Structures* 133 (December): 853–62.

<https://doi.org/10.1016/j.compstruct.2015.07.059>.

Gonzalez Henriquez, Raelvim, and Pierre Mertiny. 2018. “3.21 Filament Winding Applications.” *Comprehensive Composite Materials II*, January, 556–77.

<https://doi.org/10.1016/B978-0-12-803581-8.10313-3>.

HARRISON, A R. 2000. *A Low-Investment Cost Composites High Roof for the Ford Transit van* © ©1999 Ford Motor Co. *Integrated Design and Manufacture Using Fibre-Reinforced Polymeric Composites*. Woodhead Publishing Ltd.

<https://doi.org/10.1533/9781855738874.207>.

Jia, Xiaolong, Gang Chen, Yunhua Yu, Gang Li, Jinming Zhu, Xiangpeng Luo, Chenghong Duan, Xiaoping Yang, and David Hui. 2013. “Effect of Geometric Factor, Winding Angle and Pre-Crack Angle on Quasi-Static Crushing Behavior of Filament Wound CFRP Cylinder.” *Composites Part B: Engineering* 45 (1): 1336–43. <https://doi.org/10.1016/j.compositesb.2012.09.060>.

Joshi, S. C. 2012. *The Pultrusion Process for Polymer Matrix Composites*.

*Manufacturing Techniques for Polymer Matrix Composites (PMCs)*. Woodhead

Publishing Limited. <https://doi.org/10.1016/B978-0-85709-067-6.50012-2>.

Kannan, M., K. Kalaichelvan, and T. Sornakumar. 2015. “Development and Mechanical Testing of Filament Wound FRP Composite Components.” *Applied Mechanics and Materials* 787 (August): 578–82.

<https://doi.org/10.4028/www.scientific.net/AMM.787.578>.

Kaynak, Cevdet, E. Salim Erdiller, Levend Parnas, and Fikret Senel. 2005. “Use of Split-Disk Tests for the Process Parameters of Filament Wound Epoxy Composite Tubes.” *Polymer Testing* 24 (5): 648–55.

<https://doi.org/10.1016/j.polymertesting.2005.03.012>.

Khalifa, Ated Ben, Mondher Zidi, and Laksimi Abdelwahed. 2012. "Mechanical Characterization of Glass/Vinylester  $\pm 55^\circ$  Filament Wound Pipes by Acoustic Emission under Axial Monotonic Loading." *Comptes Rendus - Mecanique* 340 (6): 453–60. <https://doi.org/10.1016/j.crme.2012.02.006>.

Kim, Jung-Seok, Hyuk-Jin Yoon, and Kwang-Bok Shin. 2011. "A Study on Crushing Behaviors of Composite Circular Tubes with Different Reinforcing Fibers." *International Journal of Impact Engineering* 38 (4): 198–207. <https://doi.org/10.1016/j.ijimpeng.2010.11.007>.

Marco, F., and C. Gallegos. 2014. "Theoretical and Experimental Performance Analysis of a Cellular Gfrp Vehicular Bridge Deck," no. June. <https://doi.org/10.13140/RG.2.1.1737.6887>.

Martins, L.A.L., F.L. Bastian, and T.A. Netto. 2014. "Reviewing Some Design Issues for Filament Wound Composite Tubes." *Materials & Design* 55 (March): 242–49. <https://doi.org/10.1016/j.matdes.2013.09.059>.

Materials, Electrical Insulation. n.d. "Araldite Impregnating Resin System Araldite MY 740 Aradur HY 918 Accelerator DY 062 Product Data," no. November 2002.

Mertiny, P., F. Ellyin, and A. Hothan. 2004. "An Experimental Investigation on the Effect of Multi-Angle Filament Winding on the Strength of Tubular Composite Structures." *Composites Science and Technology* 64 (1): 1–9. [https://doi.org/10.1016/S0266-3538\(03\)00198-2](https://doi.org/10.1016/S0266-3538(03)00198-2).

Perillo, Giovanni, Robin Vacher, Frode Grytten, Steinar Sørbø, and Virgile Delhaye. 2014. "Material Characterisation and Failure Envelope Evaluation of Filament Wound GFRP and CFRP Composite Tubes." *Polymer Testing* 40: 54–62. <https://doi.org/10.1016/j.polymertesting.2014.08.009>.

Quanjin, Ma, M. R.M. Rejab, M. S. Idris, B. Bachtiar, J. P. Siregar, and M. N. Harith.

2017. "Design and Optimize of 3-Axis Filament Winding Machine." *IOP Conference Series: Materials Science and Engineering* 257 (1).  
<https://doi.org/10.1088/1757-899X/257/1/012039>.
- Rafiee, Roham. 2013a. "Experimental and Theoretical Investigations on the Failure of Filament Wound GRP Pipes." *Composites Part B: Engineering* 45 (1): 257–67.  
<https://doi.org/10.1016/j.compositesb.2012.04.009>.
- Rafiee. 2013b. "Apparent Hoop Tensile Strength Prediction of Glass Fiber-Reinforced Polyester Pipes." *Journal of Composite Materials* 47 (11): 1377–86.  
<https://doi.org/10.1177/0021998312447209>.
- Rafiee, Roham, and Mohammad Reza Habibagahi. 2018. "Evaluating Mechanical Performance of GFRP Pipes Subjected to Transverse Loading." *Thin-Walled Structures* 131 (March): 347–59. <https://doi.org/10.1016/j.tws.2018.06.037>.
- Rafiee, Roham, Mohammad Ali Torabi, and Sattar Maleki. 2018. "Investigating Structural Failure of a Filament-Wound Composite Tube Subjected to Internal Pressure: Experimental and Theoretical Evaluation." *Polymer Testing* 67: 322–30.  
<https://doi.org/10.1016/j.polymertesting.2018.03.020>.
- Rosenow, M. W.K. 1984. "Wind Angle Effects in Glass Fibre-Reinforced Polyester Filament Wound Pipes." *Composites* 15 (2): 144–52. [https://doi.org/10.1016/0010-4361\(84\)90727-4](https://doi.org/10.1016/0010-4361(84)90727-4).
- Rousseau, J., D. Perreux, and N. Verdière. 1999. "The Influence of Winding Patterns on the Damage Behaviour of Filament-Wound Pipes." *Composites Science and Technology* 59 (9): 1439–49. [https://doi.org/10.1016/S0266-3538\(98\)00184-5](https://doi.org/10.1016/S0266-3538(98)00184-5).
- Sofi, Tasdeeq, Stefan Neunkirchen, and Ralf Schledjewski. 2018. "Path Calculation, Technology and Opportunities in Dry Fiber Winding: A Review." *Advanced Manufacturing: Polymer and Composites Science* 4 (3): 57–72.  
<https://doi.org/10.1080/20550340.2018.1500099>.



- Srebrenkoska, Vineta, Svetlana Risteska, and Maja Mijajlovikj. 2015. "Thermal Stability and Hoop Tensile Properties of Glass Fiber Composite Pipes." *International Journal of Engineering Research & Technology* 4 (12): 297–301.
- Srebrenkoska, Vineta, S. Zhezhova, and S. Naseva. 2015. "Hoop Tensile Properties of Filament Wound Pipes." In *XII. International Machines, Technologies, Materials Congress*, 1:103–5.
- Standard, International. 2009. "ASTM - D2412" 2009 (Reapproved).
- Taib, Abdelaziz A., Rachid Boukhili, Said Achiou, Sebastien Gordon, and Hychem Boukehili. 2006. "Bonded Joints with Composite Adherends. Part I. Effect of Specimen Configuration, Adhesive Thickness, Spew Fillet and Adherend Stiffness on Fracture." *International Journal of Adhesion and Adhesives* 26 (4): 226–36.  
<https://doi.org/10.1016/j.ijadhadh.2005.03.015>.
- Tarakcioglu, Necmettin, Lokman Gemi, and Ahmet Yapıcı. 2005. "Fatigue Failure Behavior of Glass/Epoxy ±55 Filament Wound Pipes under Internal Pressure." *Composites Science and Technology* 65 (3–4): 703–8.  
<https://doi.org/10.1016/j.compscitech.2004.10.002>.